Universität Regensburg
Mathematik

On the stable numerical approximation of two-phase flow with insoluble surfactant

John W. Barrett, Harald Garcke and Robert Nürnberg

Preprint Nr. 20/2013

On the Stable Numerical Approximation of Two-Phase Flow with Insoluble Surfactant

John W. Barrett[†] Harald Garcke[‡] Robert Nürnberg[†]

Abstract

We present a parametric finite element approximation of two-phase flow with insoluble surfactant. This free boundary problem is given by the Navier–Stokes equations for the two-phase flow in the bulk, which are coupled to the transport equation for the insoluble surfactant on the interface that separates the two phases. We combine the evolving surface finite element method with an approach previously introduced by the authors for two-phase Navier–Stokes flow, which maintains good mesh properties. The derived finite element approximation of two-phase flow with insoluble surfactant can be shown to be stable. Several numerical simulations demonstrate the practicality of our numerical method.

Key words. incompressible two-phase flow, insoluble surfactants, finite elements, front tracking, ALE ESFEM

1 Introduction

The presence of surface active agents (surfactants) has a noticeable effect on the deformation of fluid-fluid interfaces, because these impurities lower the surface tension. In addition, surfactant gradients along the fluid-fluid interface cause tangential stresses leading to fluid motion (the Marangoni effect). As a result, the presence of surfactants can have a dramatic effect on droplet shapes during their evolution. Surfactants are applied in a wide range of technologies to increase the efficiency of wetting agents, detergents, foams and emulsion stabilisers.

In this paper we study the effect of an insoluble surfactant in a two-phase flow. The mathematical model consists of the Navier–Stokes equations in the two phases, together with jump conditions at the free boundary separating the two phases. In particular, the Laplace–Young condition has to hold, which is a force balance involving forces resulting from the two fluids. These forces are expressed with the help of the stress tensor as well

[†]Department of Mathematics, Imperial College London, London, SW7 2AZ, UK
[‡]Fakultät für Mathematik, Universität Regensburg, 93040 Regensburg, Germany

as surface tension forces and tangential Marangoni forces, where the latter two involve the surfactant concentration. The insoluble surfactant is transported on the interface by advection and possibly by diffusion. The overall system is quite complex, as a free boundary problem for the Navier–Stokes equations and an advection-diffusion equation on the evolving interface have to be solved simultaneously.

The mathematical analysis for the two-phase fluid flow problem with surfactants is still in its early stages. We refer to Garcke and Wieland (2006), who showed a dissipation inequality for free surface flow with an insoluble surfactant, and to Bothe *et al.* (2005, 2012); Bothe and Prüss (2010), where well-posedness and stability of equilibria for two-phase flows with soluble surfactants was shown. In particular, in Bothe and Prüss (2010) an energy inequality was crucial in order to study the stability of equilibria. In this paper, it is our aim to develop a numerical method that fulfills a discrete variant of this energy inequality and, in addition, conserves the surfactant mass and the volume of the two phases. Here we note that many of the existing numerical methods for two-phase flow with insoluble surfactant may lose mass of one of the fluid phases, or may face stability issues. In fact, to our knowledge, the numerical method presented in this paper is the first approximation of two-phase flow with insoluble surfactant in the literature that can be shown to satisfy a discrete energy law.

Different interface capturing and interface tracking methods have been used to numerically compute two-phase flows with (in-)soluble surfactants. Popular such approaches are volume of fluid methods, Renardy *et al.* (2002); James and Lowengrub (2004); Drumright-Clarke and Renardy (2004); Alke and Bothe (2009); level set methods, Xu *et al.* (2006); Teigen and Munkejord (2010); Groß and Reusken (2011); Xu *et al.* (2012); front tracking methods, Muradoglu and Tryggvason (2008); Lai *et al.* (2008); Khatri and Tornberg (2011); Xu *et al.* (2014) and arbitrary Lagrangian-Eulerian methods, Pozrikidis (2004); Yang and James (2007); Ganesan and Tobiska (2009). Another approach to model and numerically simulate two-phase fluids involving surfactants involves diffuse interface approaches and we refer to Teigen *et al.* (2009); Elliott *et al.* (2011); Garcke *et al.* (2013) and Engblom *et al.* (2013) for details.

In this work we use parametric finite elements to describe the fluid-fluid interface with an unfitted coupling to the fluid flow in the bulk, which is also discretized with the help of finite elements. Unfitted in this context means that the mesh points used to describe the interface are not, in general, mesh points of the underlying bulk finite element mesh. Our approach is based on earlier work by the authors on two-phase flow for incompressible Stokes and Navier–Stokes flow involving surface tension effects, see Barrett *et al.* (2013a,b) for details. As mentioned above, apart from capturing the interface in a two-phase flow, one also has to accurately capture the advection and diffusion of the surfactant on the interface. Here we make use of a variant of the evolving surface finite element method (ESFEM) introduced by Dziuk and Elliott (2007, 2013). In order to accurately discretize the advection-diffusion equation on the evolving interface, it is important to evolve the grid points representing the interface in such a way, that the mesh does not degenerate. In particular, it is important to avoid the coalescence of vertices or a velocity induced coarsening at parts of the interface, see e.g. Figures 2 and 3 in Section 4.

It turns out that moving vertices with the fluid velocity or with the normal part of the fluid velocity typically leads to mesh degeneracies. Hence in this paper we follow the approach from Barrett *et al.* (2013b) and allow the grid points to have a tangential velocity that is independent of the surrounding fluid motion. We note that the idea to allow for an implicit, nonzero discrete tangential velocity goes back to earlier work by the present authors, who introduced novel numerical methods with excellent mesh properties for curvature driven flows and moving boundary problems in e.g. Barrett *et al.* (2007, 2008, 2010). In fact, we are able to show that our semidiscrete continuous-in-time finite element approximations lead to *equidistributed mesh points* on the interface in two space dimensions, and to *conformal polyhedral surfaces*, which also have good mesh properties, in three space dimensions. Using this approach also ensures that, due to the good mesh properties, the surface partial differential equation for the insoluble surfactant can be solved accurately.

An important issue in surface tension driven flows is to compute curvature quantities with the help of the chosen interface representation. Our approach uses a parametric approximation of the interface, and hence we use a variant of an idea by Dziuk to compute the mean curvature. In fact Dziuk (1991) uses the identity

$$\Delta_s \, \mathrm{i}\vec{\mathrm{d}} = \vec{\varkappa}\,, \tag{1.1}$$

where Δ_s is the Laplace–Beltrami operator and $\vec{\varkappa}$ is the mean curvature vector, in a discrete setting to compute an approximation of the mean curvature. This idea was used by Bänsch (2001) for an approximation of free capillary flows, and by Bäumler and Bänsch (2013) for two-phase flows. A discretization of a variant of (1.1) was used by the present authors in Barrett *et al.* (2013a,b) to derive approximations of two-phase flow with better mesh properties. As mentioned above, this approach leads to tangential motions for the mesh points on the interface that are independent of the fluid motion. This has to be taken into account when solving the advection-diffusion equation on the interface, and in our case we naturally obtain the so-called arbitrary Lagrangian Eulerian evolving surface finite element method (ALE ESFEM), see Elliott and Styles (2012).

The structure of this article is as follows. In the next section we first state the mathematical formulation of the problem and discuss the relevant conserved quantities and an energy identity. In addition, different weak formulations are introduced which form the basis for the finite element approximations in Section 3. We state two different finite element approximations in a semidiscrete and in a fully discrete form. The first method uses the curvature discretization of Dziuk (1991) and Bänsch (2001), while the second method uses the curvature discretization introduced by the present authors in Barrett *et al.* (2007, 2008, 2013b).

Both methods, in their semidiscrete form, conserve the total surfactant concentration and allow for an energy inequality in two space dimensions. In addition, the variant based on Dziuk's curvature discretization allows for a discrete maximum principle for the surfactant approximation. On the other hand, the approach that uses the curvature discretization of the present authors leads to *good mesh properties* and to *exactly conserved volumes* of the two fluids. For the fully discrete approximations *existence and uniqueness*

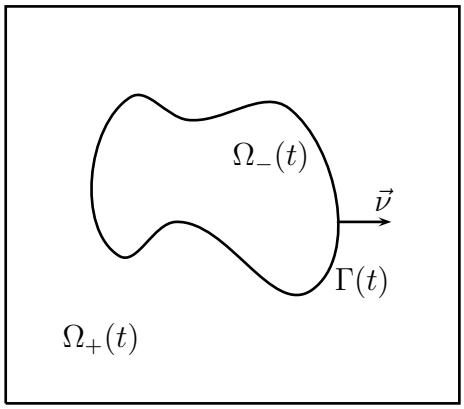

Figure 1: The domain Ω in the case $d = 2$.

as well as *conservation of the total surfactant concentration* can be shown. Finally we present several numerical simulations in two and three space dimensions in Section 4, which in particular show the effect of surfactants on the interface evolution.

2 Mathematical formulation

2.1 Governing equations

Let $\Omega \subset \mathbb{R}^d$ be a given domain, where $d = 2$ or $d = 3$. We now seek a time dependent interface $(\Gamma(t))_{t\in[0,T]}$, $\Gamma(t) \subset \Omega$, which for all $t \in [0,T]$ separates Ω into a domain $\Omega_+(t)$, occupied by one phase, and a domain $\Omega_-(t) := \Omega \setminus \overline{\Omega_+(t)}$, which is occupied by the other phase. Here the phases could represent two different liquids, or a liquid and a gas. Common examples are oil/water or water/air interfaces. See Figure 1 for an illustration. For later use, we assume that $(\Gamma(t))_{t\in[0,T]}$ is a sufficiently smooth evolving hypersurface without boundary that is parameterized by $\vec{x}(\cdot,t) : \Upsilon \to \mathbb{R}^d$, where $\Upsilon \subset \mathbb{R}^d$ is a given reference manifold, i.e. $\Gamma(t) = \vec{x}(\Upsilon, t)$. Then

$$\vec{\mathcal{V}}(\vec{z},t) := \vec{x}_t(\vec{q},t) \qquad \forall\ \vec{z} = \vec{x}(\vec{q},t) \in \Gamma(t) \tag{2.2}$$

defines the velocity of $\Gamma(t)$, and $\vec{\mathcal{V}}\,.\,\vec{\nu}$ is the normal velocity of the evolving hypersurface $\Gamma(t)$, where $\vec{\nu}(t)$ is the unit normal on $\Gamma(t)$ pointing into $\Omega_+(t)$. Moreover, we define the space-time surface

$$\mathcal{G}_T := \bigcup_{t\in[0,T]} \Gamma(t) \times \{t\}\,. \tag{2.3}$$

Let $\rho(t) = \rho_+\,\mathcal{X}_{\Omega_+(t)} + \rho_-\,\mathcal{X}_{\Omega_-(t)}$, with $\rho_\pm \in \mathbb{R}_{>0}$, denote the fluid densities, where here and throughout $\mathcal{X}_{\mathcal{A}}$ defines the characteristic function for a set $\mathcal{A}$. Denoting by $\vec{u} : \Omega \times [0,T] \to \mathbb{R}^d$ the fluid velocity, by $\underline{\underline{\sigma}} : \Omega \times [0,T] \to \mathbb{R}^{d\times d}$ the stress tensor, and by

$\vec{f}: \Omega \times [0,T] \to \mathbb{R}^d$ a possible forcing, the incompressible Navier–Stokes equations in the two phases are given by

$$\rho\,(\vec{u}_t + (\vec{u}\,.\,\nabla)\,\vec{u}) - \nabla\,.\,\underline{\underline{\sigma}} = \vec{f} := \rho\,\vec{f}_1 + \vec{f}_2 \qquad \text{in } \Omega_\pm(t)\,, \tag{2.4a}$$

$$\nabla\,.\,\vec{u} = 0 \qquad \text{in } \Omega_\pm(t)\,, \tag{2.4b}$$

$$\vec{u} = \vec{0} \qquad \text{on } \partial_1\Omega\,, \tag{2.4c}$$

$$\vec{u}\,.\,\vec{\mathrm{n}} = 0\,, \quad \underline{\underline{\sigma}}\,\vec{\mathrm{n}}\,.\,\vec{\mathrm{t}} = 0 \quad \forall\ \vec{\mathrm{t}} \in \{\vec{\mathrm{n}}\}^\perp \qquad \text{on } \partial_2\Omega\,, \tag{2.4d}$$

where $\partial\Omega = \partial_1\Omega \cup \partial_2\Omega$, with $\partial_1\Omega \cap \partial_2\Omega = \emptyset$, denotes the boundary of Ω with outer unit normal $\vec{\mathrm{n}}$ and $\{\vec{\mathrm{n}}\}^\perp := \{\vec{\mathrm{t}} \in \mathbb{R}^d : \vec{\mathrm{t}}\,.\,\vec{\mathrm{n}} = 0\}$. Hence (2.4c) prescribes a no-slip condition on $\partial_1\Omega$, while (2.4d) prescribes a free-slip condition on $\partial_2\Omega$. In addition, the stress tensor in (2.4a) is defined by

$$\underline{\underline{\sigma}} = \mu\,(\nabla\,\vec{u} + (\nabla\,\vec{u})^T) - p\,\underline{\underline{Id}} = 2\,\mu\,\underline{\underline{D}}(\vec{u}) - p\,\underline{\underline{Id}}\,, \tag{2.5}$$

where $\underline{\underline{Id}} \in \mathbb{R}^{d\times d}$ denotes the identity matrix, $\underline{\underline{D}}(\vec{u}) := \frac{1}{2}\,(\nabla\vec{u} + (\nabla\vec{u})^T)$ is the rate-of-deformation tensor, $p : \Omega \times [0,T] \to \mathbb{R}$ is the pressure and $\mu(t) = \mu_+\,\mathcal{X}_{\Omega_+(t)} + \mu_-\,\mathcal{X}_{\Omega_-(t)}$, with $\mu_\pm \in \mathbb{R}_{>0}$, denotes the dynamic viscosities in the two phases. On the free surface $\Gamma(t)$, the following conditions need to hold:

$$[\vec{u}]^+_- = \vec{0} \qquad \text{on } \Gamma(t)\,, \tag{2.6a}$$

$$[\underline{\underline{\sigma}}\,\vec{\nu}]^+_- = -\gamma(\psi)\,\varkappa\,\vec{\nu} - \nabla_s\,\gamma(\psi) \qquad \text{on } \Gamma(t)\,, \tag{2.6b}$$

$$\vec{\mathcal{V}}\,.\,\vec{\nu} = \vec{u}\,.\,\vec{\nu} \qquad \text{on } \Gamma(t)\,, \tag{2.6c}$$

where $\gamma \in C^1([0,\psi_\infty))$, with $\psi_\infty \in \mathbb{R}_{>0} \cup \{\infty\}$ and

$$\gamma'(r) \leq 0 \qquad \forall\ r \in [0,\psi_\infty)\,, \tag{2.7}$$

denotes the surface tension which depends on the surfactant concentration $\psi : \mathcal{G}_T \to [0,\psi_\infty)$, recall (2.3), and ∇_s denotes the surface gradient on $\Gamma(t)$. In addition, $\varkappa$ denotes the mean curvature of $\Gamma(t)$, i.e. the sum of the principal curvatures of $\Gamma(t)$, where we have adopted the sign convention that $\varkappa$ is negative where $\Omega_-(t)$ is locally convex. In particular, on letting $\vec{\mathrm{id}}$ denote the identity function in $\mathbb{R}^d$, it holds that

$$\Delta_s\,\vec{\mathrm{id}} = \varkappa\,\vec{\nu} =: \vec{\varkappa} \qquad \text{on } \Gamma(t)\,, \tag{2.8}$$

where $\Delta_s = \nabla_s\,.\,\nabla_s$ is the Laplace–Beltrami operator on $\Gamma(t)$, with $\nabla_s\,.$ denoting surface divergence on $\Gamma(t)$. Moreover, as usual, $[\vec{u}]^+_- := \vec{u}_+ - \vec{u}_-$ and $[\underline{\underline{\sigma}}\,\vec{\nu}]^+_- := \underline{\underline{\sigma}}_+\,\vec{\nu} - \underline{\underline{\sigma}}_-\,\vec{\nu}$ denote the jumps in velocity and normal stress across the interface $\Gamma(t)$. Here and throughout, we employ the shorthand notation $\vec{g}_\pm := \vec{g}\,|_{\Omega_\pm(t)}$ for a function $\vec{g} : \Omega \times [0,T] \to \mathbb{R}^d$; and similarly for scalar and matrix-valued functions. The surfactant transport (with diffusion) on $\Gamma(t)$ is then given by

$$\partial_t^\bullet\,\psi + \psi\,\nabla_s\,.\vec{u} - \nabla_s\,.\,(\mathcal{D}_\Gamma\,\nabla_s\,\psi) = 0 \qquad \text{on } \Gamma(t)\,, \tag{2.9}$$

where $\mathcal{D}_\Gamma \geq 0$ is a diffusion coefficient, and where

$$\partial_t^\bullet\,\zeta = \zeta_t + \vec{u}\,.\,\nabla\,\zeta \qquad \forall\ \zeta \in H^1(\mathcal{G}_T) \tag{2.10}$$

denotes the material time derivative of ζ on $\Gamma(t)$. Here we stress that the derivative in (2.10) is well-defined, and depends only on the values of ζ on $\mathcal{G}_T$, even though ζ_t and $\nabla\zeta$ do not make sense separately; see e.g. Dziuk and Elliott (2013, p. 324). The system (2.4a–d), (2.5), (2.6a–c), (2.9) is closed with the initial conditions

$$\Gamma(0) = \Gamma_0\,, \qquad \psi(\cdot,0) = \psi_0 \qquad \text{on } \Gamma_0\,, \qquad \vec{u}(\cdot,0) = \vec{u}_0 \qquad \text{in } \Omega\,, \tag{2.11}$$

where $\Gamma_0 \subset \Omega$, $\vec{u}_0 : \Omega \to \mathbb{R}^d$ and $\psi_0 : \Gamma_0 \to [0,\psi_\infty)$ are given initial data.

For later purposes, we introduce the surface energy function F, which satisfies

$$\gamma(r) = F(r) - r\,F'(r) \qquad \forall\ r \in (0,\psi_\infty)\,, \tag{2.12a}$$

and

$$\lim_{r\to 0} r\,F'(r) = F(0) - \gamma(0) = 0\,. \tag{2.12b}$$

This means in particular that

$$\gamma'(r) = -r\,F''(r) \qquad \forall\ r \in (0,\psi_\infty)\,. \tag{2.13}$$

It immediately follows from (2.13) and (2.7) that $F \in C([0,\psi_\infty)) \cap C^2(0,\psi_\infty)$ is convex. Typical examples for γ and F are given by

$$\gamma(r) = \gamma_0\,(1-\beta\,r)\,, \quad F(r) = \gamma_0\,[1+\beta\,r\,(\ln r - 1)]\ ,\ \psi_\infty = \infty\,, \tag{2.14a}$$

which represents a linear equation of state, and by

$$\gamma(r) = \gamma_0\left[1+\beta\,\psi_\infty\,\ln\left(1-\tfrac{r}{\psi_\infty}\right)\right], \quad F(r) = \gamma_0\left[1+\beta\left(r\,\ln\tfrac{r}{\psi_\infty - r} + \psi_\infty\,\ln\tfrac{\psi_\infty - r}{\psi_\infty}\right)\right], \tag{2.14b}$$

the so-called Langmuir equation of state, where $\gamma_0 \in \mathbb{R}_{>0}$ and $\beta \in \mathbb{R}_{\geq 0}$ are further given parameters, where we note that the special case $\beta = 0$ means that (2.14a,b) reduce to

$$F(r) = \gamma(r) = \gamma_0 \in \mathbb{R}_{>0} \qquad \forall\ r \in \mathbb{R}\,. \tag{2.15}$$

Moreover, we observe that (2.14a) can be viewed as a linearization of (2.14b) in the sense that γ in (2.14a) is affine, and γ and γ' agree at the origin with γ and γ' from (2.14b).

2.2 Weak formulation

Before introducing our finite element approximation, we will state an appropriate weak formulation. With this in mind, we introduce the function spaces

$$\mathbb{U} := \{\vec{\varphi} \in [H^1(\Omega)]^d : \vec{\varphi} = \vec{0} \ \text{ on } \partial_1\Omega\,,\ \vec{\varphi}\,.\,\vec{n} = 0 \text{ a.e. on } \partial_2\Omega\}\,, \quad \mathbb{P} := L^2(\Omega)\,,$$
$$\widehat{\mathbb{P}} := \{\eta \in \mathbb{P} : \int_\Omega \eta\,\mathrm{d}\mathcal{L}^d = 0\}\,, \quad \mathbb{V} := L^2(0,T;\mathbb{U}) \cap H^1(0,T;[L^2(\Omega)]^d)\,, \quad \mathbb{S} := H^1(\mathcal{G}_T)\,.$$

Let $(\cdot,\cdot)$ and $\langle\cdot,\cdot\rangle_{\Gamma(t)}$ denote the L^2–inner products on Ω and $\Gamma(t)$, respectively. We recall from Barrett *et al.* (2013b) that it follows from (2.4b–d) and (2.6c) that

$$(\rho\,(\vec{u}\,.\,\nabla)\,\vec{u},\vec{\xi}) = \tfrac{1}{2}\left[(\rho\,(\vec{u}\,.\,\nabla)\,\vec{u},\vec{\xi}) - (\rho\,(\vec{u}\,.\,\nabla)\,\vec{\xi},\vec{u}) - \left\langle [\rho]^+_-\,\vec{u}\,.\,\vec{\nu},\vec{u}\,.\,\vec{\xi}\right\rangle_{\Gamma(t)}\right] \qquad \forall\ \vec{\xi}\in[H^1(\Omega)]^d \quad (2.16)$$

and

$$\frac{\mathrm{d}}{\mathrm{d}t}(\rho\,\vec{u},\vec{\xi}) = (\rho\,\vec{u}_t,\vec{\xi}) + (\rho\,\vec{u},\vec{\xi}_t) - \left\langle [\rho]^+_-\,\vec{u}\,.\,\vec{\nu},\vec{u}\,.\,\vec{\xi}\right\rangle_{\Gamma(t)} \qquad \forall\ \vec{\xi}\in\mathbb{V}\,,$$

respectively. Therefore, it holds that

$$(\rho\,\vec{u}_t,\vec{\xi}) = \tfrac{1}{2}\left[\frac{\mathrm{d}}{\mathrm{d}t}(\rho\,\vec{u},\vec{\xi}) + (\rho\,\vec{u}_t,\vec{\xi}) - (\rho\,\vec{u},\vec{\xi}_t) + \left\langle [\rho]^+_-\,\vec{u}\,.\,\vec{\nu},\vec{u}\,.\,\vec{\xi}\right\rangle_{\Gamma(t)}\right] \qquad \forall\ \vec{\xi}\in\mathbb{V}\,,$$

which on combining with (2.16) yields that

$$\begin{aligned}&(\rho\,[\vec{u}_t + (\vec{u}\,.\,\nabla)\,\vec{u}],\vec{\xi})\\ &\quad = \tfrac{1}{2}\left[\frac{\mathrm{d}}{\mathrm{d}t}(\rho\,\vec{u},\vec{\xi}) + (\rho\,\vec{u}_t,\vec{\xi}) - (\rho\,\vec{u},\vec{\xi}_t) + (\rho,[(\vec{u}\,.\,\nabla)\,\vec{u}]\,.\,\vec{\xi} - [(\vec{u}\,.\,\nabla)\,\vec{\xi}]\,.\,\vec{u})\right] \quad \forall\ \vec{\xi}\in\mathbb{V}\,.\end{aligned} \tag{2.17}$$

Moreover, it holds on noting (2.4d) and (2.6b) that for all $\vec{\xi}\in\mathbb{U}$

$$\int_{\Omega_+(t)\cup\Omega_-(t)} (\nabla\,.\,\underline{\underline{\sigma}})\,.\,\vec{\xi}\,\mathrm{d}\mathcal{L}^d = -2\,(\mu\,\underline{\underline{D}}(\vec{u}),\underline{\underline{D}}(\vec{\xi})) + (p,\nabla\,.\,\vec{\xi}) + \left\langle \gamma(\psi)\,\varkappa\,\vec{\nu} + \nabla_s\,\gamma(\psi),\vec{\xi}\right\rangle_{\Gamma(t)}. \tag{2.18}$$

Similarly to (2.10) we define the following time derivative that follows the parameterization $\vec{x}(\cdot,t)$ of $\Gamma(t)$, rather than $\vec{u}$. In particular, we let

$$\partial^\circ_t\,\zeta = \zeta_t + \vec{\mathcal{V}}\,.\,\nabla\,\zeta \qquad \forall\ \zeta\in\mathbb{S}\,, \tag{2.19}$$

recall (2.2). Here we stress once again that this definition is well-defined, even though ζ_t and $\nabla\,\zeta$ do not make sense separately for a function $\zeta\in\mathbb{S}$. On recalling (2.10) we obtain that

$$\partial^\circ_t = \partial^\bullet_t \qquad \text{if} \qquad \vec{\mathcal{V}} = \vec{u} \quad \text{on } \Gamma(t)\,. \tag{2.20}$$

We note that the definition (2.19) differs from the definition of ∂° in Dziuk and Elliott (2013, p. 327), where $\partial^\circ\,\zeta = \zeta_t + (\vec{\mathcal{V}}\,.\,\vec{\nu})\,\vec{\nu}\,.\,\nabla\,\zeta$ for the "normal time derivative". It holds that

$$\frac{\mathrm{d}}{\mathrm{d}t}\,\langle\chi,\zeta\rangle_{\Gamma(t)} = \langle\partial^\circ_t\,\chi,\zeta\rangle_{\Gamma(t)} + \langle\chi,\partial^\circ_t\,\zeta\rangle_{\Gamma(t)} + \left\langle\chi\,\zeta,\nabla_s\,.\,\vec{\mathcal{V}}\right\rangle_{\Gamma(t)} \qquad \forall\ \chi,\zeta\in\mathbb{S}\,, \tag{2.21}$$

see Dziuk and Elliott (2013, Lem. 5.2), and that

$$\langle\zeta,\nabla_s\,.\,\vec{\eta}\rangle_{\Gamma(t)} + \langle\nabla_s\,\zeta,\vec{\eta}\rangle_{\Gamma(t)} = -\,\langle\zeta\,\vec{\eta},\vec{\varkappa}\rangle_{\Gamma(t)} \qquad \forall\ \zeta\in H^1(\Gamma(t)),\ \vec{\eta}\in[H^1(\Gamma(t))]^d\,, \tag{2.22}$$

see Dziuk and Elliott (2013, Def. 2.11). For later use we remark that it follows from (2.22) that

$$\left\langle \gamma(\psi)\,\vec{\varkappa} + \nabla_s\,\gamma(\psi), \vec{\xi} \right\rangle_{\Gamma(t)} = \left\langle \gamma(\psi)\,\varkappa\,\vec{\nu} + \nabla_s\,\gamma(\psi), \vec{\xi} \right\rangle_{\Gamma(t)} = -\left\langle \gamma(\psi), \nabla_s\,.\,\vec{\xi} \right\rangle_{\Gamma(t)} \quad \forall\ \vec{\xi} \in \mathbb{U}\,. \tag{2.23}$$

The natural weak formulation of the system (2.4a–d), (2.5), (2.6a–c), (2.9) is then given as follows. Find $\Gamma(t) = \vec{x}(\Upsilon, t)$ for $t \in [0,T]$ with $\vec{\mathcal{V}} \in L^2(0,T;[H^1(\Gamma(t))]^d)$, and functions $\vec{u} \in \mathbb{V}$, $p \in L^2(0,T;\widehat{\mathbb{P}})$, $\vec{\varkappa} \in L^2(0,T;[L^2(\Gamma(t))]^d)$ and $\psi \in \mathbb{S}$ such that for almost all $t \in (0,T)$ it holds that

$$\begin{aligned} &\tfrac{1}{2}\left[\frac{\mathrm{d}}{\mathrm{d}t}(\rho\,\vec{u},\vec{\xi}) + (\rho\,\vec{u}_t,\vec{\xi}) - (\rho\,\vec{u},\vec{\xi}_t) + (\rho,[(\vec{u}\,.\,\nabla)\,\vec{u}]\,.\,\vec{\xi} - [(\vec{u}\,.\,\nabla)\,\vec{\xi}]\,.\,\vec{u})\right] \\ &\qquad + 2\,(\mu\,\underline{\underline{D}}(\vec{u}),\underline{\underline{D}}(\vec{\xi})) - (p,\nabla\,.\,\vec{\xi}) - \left\langle \gamma(\psi)\,\vec{\varkappa} + \nabla_s\,\gamma(\psi), \vec{\xi} \right\rangle_{\Gamma(t)} = (\vec{f},\vec{\xi}) \qquad \forall\ \vec{\xi} \in \mathbb{V}\,, \end{aligned} \tag{2.24a}$$

$$(\nabla\,.\,\vec{u},\varphi) = 0 \qquad \forall\ \varphi \in \widehat{\mathbb{P}}\,, \tag{2.24b}$$

$$\left\langle \vec{\mathcal{V}} - \vec{u}, \vec{\chi} \right\rangle_{\Gamma(t)} = 0 \qquad \forall\ \vec{\chi} \in [L^2(\Gamma(t))]^d\,, \tag{2.24c}$$

$$\langle \vec{\varkappa}, \vec{\eta} \rangle_{\Gamma(t)} + \left\langle \nabla_s\,\mathrm{i}\vec{\mathrm{d}}, \nabla_s\,\vec{\eta} \right\rangle_{\Gamma(t)} = 0 \qquad \forall\ \vec{\eta} \in [H^1(\Gamma(t))]^d\,, \tag{2.24d}$$

$$\frac{\mathrm{d}}{\mathrm{d}t}\,\langle \psi,\zeta \rangle_{\Gamma(t)} + \mathcal{D}_\Gamma\,\langle \nabla_s\,\psi, \nabla_s\,\zeta \rangle_{\Gamma(t)} = \langle \psi, \partial_t^\circ\,\zeta \rangle_{\Gamma(t)} \quad \forall\ \zeta \in \mathbb{S}\,, \tag{2.24e}$$

as well as the initial conditions (2.11), where in (2.24c) we have recalled (2.2). Here (2.24a–d) can be derived analogously to the weak formulation presented in Barrett *et al.* (2013b), recall (2.17) and (2.18), while (2.24e) is a direct consequence of (2.21) and (2.22); see Dziuk and Elliott (2013). Of course, it follows from (2.24c) and (2.20) that ∂_t° in (2.24e) can be replaced by $\partial_t^\bullet$.

REMARK. 2.1. *For ease of presentation, in this paper we restrict ourselves to the case of two-phase Navier–Stokes flow, i.e.* $\rho_\pm > 0$. *However, it is a simple matter to generalize the results in this paper to two-phase Stokes flow in the bulk, i.e. to* $\rho_+ = \rho_- = 0$. *For example, the weak formulation* (2.24a–e) *then holds with* $\rho = 0$ *and with* $\mathbb{V}$ *replaced by* $L^2(0,T;\mathbb{U})$*; and analogous simplifications can be applied to the finite element approximations that will be introduced later in this paper, see also Barrett* et al. *(2013a). For example, the presented fully discrete schemes in §3.2 are valid for arbitrary choices of* $\rho_\pm \geq 0$.

2.3 Energy bounds

In what follows we would like to derive an energy bound for a solution of (2.24a–e). All of the following considerations are formal, in the sense that we make the appropriate assumptions about the existence, boundedness and regularity of a solution to (2.24a–e). In particular, we assume that $\psi \in [0,\psi_\infty)$. Choosing $\vec{\xi} = \vec{u}$ in (2.24a) and $\varphi = p(\cdot,t)$ in

(2.24b) yields that

$$\tfrac{1}{2}\,\frac{\mathrm{d}}{\mathrm{d}t}\,\|\rho^{\frac{1}{2}}\,\vec{u}\|_0^2 + 2\,\|\mu^{\frac{1}{2}}\,\underline{\underline{D}}(\vec{u})\|_0^2 = (\vec{f},\vec{u}) + \langle\gamma(\psi)\,\vec{\varkappa} + \nabla_s\,\gamma(\psi),\vec{u}\rangle_{\Gamma(t)}\,. \tag{2.25}$$

In what follows, assuming that γ is not constant, recall (2.15), we would like to choose $\zeta = F'(\psi)$ in (2.24e). As F' in general is singular at the origin, recall (2.13), we instead choose $\zeta = F'(\psi+\alpha)$ for some $\alpha \in \mathbb{R}_{>0}$ with $\psi + \alpha < \psi_\infty$. Then we obtain, on recalling (2.12a) and (2.21), that

$$\begin{aligned}\frac{\mathrm{d}}{\mathrm{d}t}\,\langle F(\psi+\alpha) - \gamma(\psi+\alpha),1\rangle_{\Gamma(t)} + \mathcal{D}_\Gamma\,\langle\nabla_s\,(\psi+\alpha),\nabla_s\,F'(\psi+\alpha)\rangle_{\Gamma(t)}\\ = \langle\psi+\alpha,\partial_t^\circ\,F'(\psi+\alpha)\rangle_{\Gamma(t)} + \alpha\left\langle F'(\psi+\alpha),\nabla_s\,.\,\vec{\mathcal{V}}\right\rangle_{\Gamma(t)}\,.\end{aligned} \tag{2.26}$$

Moreover, choosing $\chi = \gamma(\psi+\alpha)$, $\zeta = 1$ in (2.21), and then choosing $\vec{\eta} = \vec{\mathcal{V}}$, $\zeta = \gamma(\psi+\alpha)$ in (2.22) leads to

$$\begin{aligned}\frac{\mathrm{d}}{\mathrm{d}t}\,\langle\gamma(\psi+\alpha),1\rangle_{\Gamma(t)} &= \langle\partial_t^\circ\,\gamma(\psi+\alpha),1\rangle_{\Gamma(t)} + \left\langle\gamma(\psi+\alpha),\nabla_s\,.\,\vec{\mathcal{V}}\right\rangle_{\Gamma(t)}\\ &= \langle\partial_t^\circ\,\gamma(\psi+\alpha),1\rangle_{\Gamma(t)} - \left\langle\gamma(\psi+\alpha)\,\vec{\varkappa} + \nabla_s\,\gamma(\psi+\alpha),\vec{\mathcal{V}}\right\rangle_{\Gamma(t)}\,.\end{aligned} \tag{2.27}$$

In addition, it follows from (2.13) that

$$\partial_t^\circ\,\gamma(\psi+\alpha) = \gamma'(\psi+\alpha)\,\partial_t^\circ\,\psi = -(\psi+\alpha)\,F''(\psi+\alpha)\,\partial_t^\circ\,\psi = -(\psi+\alpha)\,\partial_t^\circ\,F'(\psi+\alpha)\,. \tag{2.28}$$

Combining (2.26), (2.27) and (2.28) yields that

$$\begin{aligned}\frac{\mathrm{d}}{\mathrm{d}t}\,\langle F(\psi+\alpha),1\rangle_{\Gamma(t)} + \mathcal{D}_\Gamma\,\langle\nabla_s\,\mathcal{F}(\psi+\alpha),\nabla_s\,\mathcal{F}(\psi+\alpha)\rangle_{\Gamma(t)}\\ = -\left\langle\gamma(\psi+\alpha)\,\vec{\varkappa} + \nabla_s\,\gamma(\psi+\alpha),\vec{\mathcal{V}}\right\rangle_{\Gamma(t)} + \alpha\left\langle F'(\psi+\alpha),\nabla_s\,.\,\vec{\mathcal{V}}\right\rangle_{\Gamma(t)}\,,\end{aligned} \tag{2.29}$$

where, on recalling (2.13) and (2.7),

$$\mathcal{F}(r) = \int_0^r [F''(y)]^{\frac{1}{2}}\,\mathrm{d}y\,.$$

Letting $\alpha \to 0$ in (2.29) yields, on recalling (2.12b), that

$$\frac{\mathrm{d}}{\mathrm{d}t}\,\langle F(\psi),1\rangle_{\Gamma(t)} + \mathcal{D}_\Gamma\,\langle\nabla_s\,\mathcal{F}(\psi),\nabla_s\,\mathcal{F}(\psi)\rangle_{\Gamma(t)} = -\left\langle\gamma(\psi)\,\vec{\varkappa} + \nabla_s\,\gamma(\psi),\vec{\mathcal{V}}\right\rangle_{\Gamma(t)}\,. \tag{2.30}$$

We note that (2.30) is still valid in the case (2.15), on noting (2.21) and (2.23). Combining (2.30) with (2.25) implies the a priori energy equation

$$\frac{\mathrm{d}}{\mathrm{d}t}\left(\tfrac{1}{2}\,\|\rho^{\frac{1}{2}}\,\vec{u}\|_0^2 + \langle F(\psi),1\rangle_{\Gamma(t)}\right) + 2\,\|\mu^{\frac{1}{2}}\,\underline{\underline{D}}(\vec{u})\|_0^2 + \mathcal{D}_\Gamma\,\langle\nabla_s\,\mathcal{F}(\psi),\nabla_s\,\mathcal{F}(\psi)\rangle_{\Gamma(t)} = (\vec{f},\vec{u})\,. \tag{2.31}$$

Moreover, the volume of $\Omega_-(t)$ is preserved in time, i.e. the mass of each phase is conserved. To see this, choose $\vec{\chi} = \vec{\nu}$ in (2.24c) and $\varphi = \mathcal{X}_{\Omega_-(t)}$ in (2.24b) to obtain

$$\frac{\mathrm{d}}{\mathrm{d}t}\mathcal{L}^d(\Omega_-(t)) = \left\langle \vec{\mathcal{V}}, \vec{\nu} \right\rangle_{\Gamma(t)} = \langle \vec{u}, \vec{\nu} \rangle_{\Gamma(t)} = \int_{\Omega_-(t)} \nabla \,.\, \vec{u} \,\mathrm{d}\mathcal{L}^d = 0\,. \tag{2.32}$$

In addition, we note that it immediately follows from choosing $\zeta = 1$ in (2.24e) that the total amount of surfactant is preserved, i.e.

$$\frac{\mathrm{d}}{\mathrm{d}t}\int_{\Gamma(t)} \psi \,\mathrm{d}\mathcal{H}^{d-1} = 0\,. \tag{2.33}$$

2.4 Alternative weak formulation

It will turn out that another weak formulation of the overall system (2.4a–d), (2.5), (2.6a–c), (2.9) will lead to finite element approximations with better mesh properties. In order to derive the weak formulation, and on recalling (2.20), we note that if we relax $\vec{\mathcal{V}} = \vec{u}|_{\Gamma(t)}$ to

$$\vec{\mathcal{V}} \,.\, \vec{\nu} = \vec{u} \,.\, \vec{\nu} \quad \text{on } \Gamma(t)\,,$$

then it holds that

$$\partial_t^\circ \,\zeta = \partial_t^\bullet \,\zeta + (\vec{\mathcal{V}} - \vec{u}) \,.\, \nabla_s \,\zeta \qquad \forall\ \zeta \in \mathbb{S}\,. \tag{2.34}$$

Our preferred finite element approximation will then be based on the following weak formulation. Find $\Gamma(t) = \vec{x}(\Upsilon, t)$ for $t \in [0,T]$ with $\vec{\mathcal{V}} \in L^2(0,T;[H^1(\Gamma(t))]^d)$, and functions $\vec{u} \in \mathbb{V}$, $p \in L^2(0,T;\widehat{\mathbb{P}})$, $\varkappa \in L^2(0,T;L^2(\Gamma(t)))$ and $\psi \in \mathbb{S}$ such that for almost all $t \in (0,T)$ it holds that

$$\begin{aligned}
&\tfrac{1}{2}\left[\frac{\mathrm{d}}{\mathrm{d}t}(\rho\,\vec{u},\vec{\xi}) + (\rho\,\vec{u}_t,\vec{\xi}) - (\rho\,\vec{u},\vec{\xi}_t) + (\rho,[(\vec{u}\,.\,\nabla)\,\vec{u}]\,.\,\vec{\xi} - [(\vec{u}\,.\,\nabla)\,\vec{\xi}]\,.\,\vec{u})\right] \\
&\qquad + 2\,(\mu\,\underline{\underline{D}}(\vec{u}),\underline{\underline{D}}(\vec{\xi})) - (p,\nabla\,.\,\vec{\xi}) - \left\langle \gamma(\psi)\,\varkappa\,\vec{\nu} + \nabla_s\,\gamma(\psi),\vec{\xi}\right\rangle_{\Gamma(t)} = (\vec{f},\vec{\xi}) \qquad \forall\ \vec{\xi} \in \mathbb{V}\,,
\end{aligned} \tag{2.35a}$$

$$(\nabla\,.\,\vec{u},\varphi) = 0 \qquad \forall\ \varphi \in \widehat{\mathbb{P}}\,, \tag{2.35b}$$

$$\left\langle \vec{\mathcal{V}} - \vec{u}, \chi\,\vec{\nu}\right\rangle_{\Gamma(t)} = 0 \qquad \forall\ \chi \in L^2(\Gamma(t))\,, \tag{2.35c}$$

$$\langle \varkappa\,\vec{\nu},\vec{\eta}\rangle_{\Gamma(t)} + \left\langle \nabla_s\,\mathrm{i}\vec{\mathrm{d}}, \nabla_s\,\vec{\eta}\right\rangle_{\Gamma(t)} = 0 \qquad \forall\ \vec{\eta} \in [H^1(\Gamma(t))]^d\,, \tag{2.35d}$$

$$\frac{\mathrm{d}}{\mathrm{d}t}\,\langle\psi,\zeta\rangle_{\Gamma(t)} + \mathcal{D}_\Gamma\,\langle\nabla_s\,\psi,\nabla_s\,\zeta\rangle_{\Gamma(t)} + \left\langle \psi\,(\vec{\mathcal{V}} - \vec{u}),\nabla_s\,\zeta\right\rangle_{\Gamma(t)} = \langle\psi,\partial_t^\circ\,\zeta\rangle_{\Gamma(t)} \qquad \forall\ \zeta \in \mathbb{S}\,, \tag{2.35e}$$

as well as the initial conditions (2.11), where in (2.35c,e) we have recalled (2.2). The derivation of (2.35a–d) is analogous to the derivation of (2.24a–d), while for the formula-

tion (2.35e) we note (2.21) and, on recalling (2.22) and (2.34), the identity

$$\begin{aligned}\left\langle \partial_t^\circ\,\psi+\psi\,\nabla_s\,.\,\vec{\mathcal{V}},\zeta\right\rangle_{\Gamma(t)} &= \langle \partial_t^\bullet\,\psi+\psi\,\nabla_s\,.\,\vec{u},\zeta\rangle_{\Gamma(t)}+\left\langle (\vec{\mathcal{V}}-\vec{u})\,.\,\nabla_s\,\psi+\psi\,\nabla_s\,.\,(\vec{\mathcal{V}}-\vec{u}),\zeta\right\rangle_{\Gamma(t)}\\ &= \langle \partial_t^\bullet\,\psi+\psi\,\nabla_s\,.\,\vec{u},\zeta\rangle_{\Gamma(t)}-\left\langle \psi\,(\vec{\mathcal{V}}-\vec{u}),\nabla_s\,\zeta\right\rangle_{\Gamma(t)}\,,\end{aligned}$$

where we have used the fact that $\langle\vec{\mathcal{V}}-\vec{u},\psi\,\zeta\,\vec{\varkappa}\rangle_{\Gamma(t)}=0$ due to (2.35c). In fact, a simpler way of seeing that (2.35e) is consistent with (2.24e) is to recall that the latter holds with ∂_t° replaced by $\partial_t^\bullet$, and so the desired result follows immediately from (2.34).

The main differences between (2.24a–e) and (2.35a–e) are that for the latter the scalar curvature $\varkappa$ is sought as part of the solution, rather than $\vec{\varkappa}$, that in the latter only the normal part of $\vec{u}$ affects the evolution of the parameterization $\vec{x}$, and that as a consequence the weak formulation of the advection-diffusion has to account for the additional freedom in the tangential velocity of the interface parameterization.

Similarly to (2.25)–(2.31), we can formally show that a solution to (2.35a–e) satisfies the a priori energy bound (2.31). First of all we note that since $\vec{\varkappa}=\varkappa\,\vec{\nu}$, a solution to (2.35a–e) satisfies (2.25). Secondly we observe that the analogue of (2.30) has as right hand side

$$\begin{aligned}&-\left\langle\gamma(\psi)\,\vec{\varkappa}+\nabla_s\,\gamma(\psi),\vec{\mathcal{V}}\right\rangle_{\Gamma(t)}-\left\langle\psi\,(\vec{\mathcal{V}}-\vec{u}),\nabla_s\,F'(\psi)\right\rangle_{\Gamma(t)}\\ &\quad=-\left\langle\gamma(\psi)\,\varkappa\,\vec{\nu}+\nabla_s\,\gamma(\psi),\vec{\mathcal{V}}\right\rangle_{\Gamma(t)}+\left\langle\nabla_s\,\gamma(\psi),\vec{\mathcal{V}}-\vec{u}\right\rangle_{\Gamma(t)}\\ &\quad=-\langle\gamma(\psi)\,\varkappa\,\vec{\nu}+\nabla_s\,\gamma(\psi),\vec{u}\rangle_{\Gamma(t)}\,,\end{aligned}\tag{2.36}$$

where we have used (2.13) and (2.35c) with $\chi=\gamma(\psi)\,\varkappa$. Of course, (2.36) now cancels with the last term in (2.25), and so we obtain (2.31). Moreover, the properties (2.32) and (2.33) also hold.

3 Finite element approximation

3.1 Semi-discrete approximation

For simplicity we consider Ω to be a polyhedral domain. Then let $\mathcal{T}^h$ be a regular partitioning of Ω into disjoint open simplices o_j^h, $j=1,\ldots,J_\Omega^h$. Associated with $\mathcal{T}^h$ are the finite element spaces

$$S_k^h:=\{\chi\in C(\overline{\Omega}):\chi\,|_o\in\mathcal{P}_k(o)\quad\forall\,o\in\mathcal{T}^h\}\subset H^1(\Omega)\,,\qquad k\in\mathbb{N}\,,$$

where $\mathcal{P}_k(o)$ denotes the space of polynomials of degree k on o. We also introduce S_0^h, the space of piecewise constant functions on $\mathcal{T}^h$. Let $\{\varphi_{k,j}^h\}_{j=1}^{K_k^h}$ be the standard basis functions for S_k^h, $k\geq 0$. We introduce $\vec{I}_k^h:[C(\overline{\Omega})]^d\to[S_k^h]^d$, $k\geq 1$, the standard

interpolation operators, such that $(\vec{I}_k^h\,\vec{\eta})(\vec{p}_{k,j}^{\,h}) = \vec{\eta}(\vec{p}_{k,j}^{\,h})$ for $j = 1, \ldots, K_k^h$; where $\{\vec{p}_{k,j}^{\,h}\}_{j=1}^{K_k^h}$ denotes the coordinates of the degrees of freedom of S_k^h, $k \geq 1$. In addition we define the standard projection operator $I_0^h : L^1(\Omega) \to S_0^h$, such that

$$(I_0^h \eta)\,|_o = \frac{1}{\mathcal{L}^d(o)} \int_o \eta \,\mathrm{d}\mathcal{L}^d \qquad \forall\ o \in \mathcal{T}^h\,.$$

Our approximation to the velocity and pressure on $\mathcal{T}^h$ will be finite element spaces $\mathbb{U}^h \subset \mathbb{U}$ and $\mathbb{P}^h(t) \subset \mathbb{P}$. We require also the space $\widehat{\mathbb{P}}^h(t) := \mathbb{P}^h(t) \cap \widehat{\mathbb{P}}$. Based on the authors' earlier work in Barrett *et al.* (2013a,b), we will select velocity/pressure finite element spaces that satisfy the LBB inf-sup condition, see e.g. Girault and Raviart (1986, p. 114), and augment the pressure space by a single additional basis function, namely by the characteristic function of the inner phase. For the obtained spaces $(\mathbb{U}^h, \mathbb{P}^h(t))$ we are unable to prove that they satisfy an LBB condition. The extension of the given pressure finite element space, which is an example of an XFEM approach, leads to exact volume conservation of the two phases within the finite element framework. For the non-augmented spaces we may choose, for example, the lowest order Taylor–Hood element P2–P1, the P2–P0 element or the P2–(P1+P0) element on setting $\mathbb{U}^h = [S_2^h]^d \cap \mathbb{U}$, and $\mathbb{P}^h = S_1^h$, S_0^h or $S_1^h + S_0^h$, respectively. We refer to Barrett *et al.* (2013a,b) for more details.

The parametric finite element spaces in order to approximate $\vec{x}$, as well as $\vec{\varkappa}$ and $\varkappa$ in (2.24a–e) and (2.35a–e), respectively, are defined as follows. Similarly to Barrett *et al.* (2008), let $\Gamma^h(t) \subset \mathbb{R}^d$ be a $(d-1)$-dimensional *polyhedral surface*, i.e. a union of non-degenerate $(d-1)$-simplices with no hanging vertices (see Deckelnick *et al.* (2005, p. 164) for $d = 3$), approximating the closed surface $\Gamma(t)$. In particular, let $\Gamma^h(t) = \bigcup_{j=1}^{J_\Gamma} \overline{\sigma_j^h(t)}$, where $\{\sigma_j^h(t)\}_{j=1}^{J_\Gamma}$ is a family of mutually disjoint open $(d-1)$-simplices with vertices $\{\vec{q}_k^{\,h}(t)\}_{k=1}^{K_\Gamma}$. Then let

$$\begin{aligned}\underline{V}(\Gamma^h(t)) &:= \{\vec{\chi} \in [C(\Gamma^h(t))]^d : \vec{\chi}\,|_{\sigma_j^h} \text{ is linear } \forall\ j = 1, \ldots, J_\Gamma\}\\ &=: [W(\Gamma^h(t))]^d \subset [H^1(\Gamma^h(t))]^d\,,\end{aligned}$$

where $W(\Gamma^h(t)) \subset H^1(\Gamma^h(t))$ is the space of scalar continuous piecewise linear functions on $\Gamma^h(t)$, with $\{\chi_k^h(\cdot,t)\}_{k=1}^{K_\Gamma}$ denoting the standard basis of $W(\Gamma^h(t))$, i.e.

$$\chi_k^h(\vec{q}_l^{\,h}(t), t) = \delta_{kl} \qquad \forall\ k, l \in \{1, \ldots, K_\Gamma\}\,, t \in [0,T]\,. \tag{3.1}$$

For later purposes, we also introduce $\pi^h(t) : C(\Gamma^h(t)) \to W(\Gamma^h(t))$, the standard interpolation operator at the nodes $\{\vec{q}_k^{\,h}(t)\}_{k=1}^{K_\Gamma}$, and similarly $\vec{\pi}^h(t) : [C(\Gamma^h(t))]^d \to \underline{V}(\Gamma^h(t))$.

For scalar and vector functions η, ζ on $\Gamma^h(t)$ we introduce the L^2–inner product $\langle\cdot,\cdot\rangle_{\Gamma^h(t)}$ over the polyhedral surface $\Gamma^h(t)$ as follows

$$\langle \eta, \zeta \rangle_{\Gamma^h(t)} := \int_{\Gamma^h(t)} \eta\,.\,\zeta \,\mathrm{d}\mathcal{H}^{d-1}\,.$$

If η, ζ are piecewise continuous, with possible jumps across the edges of $\{\sigma_j^h\}_{j=1}^{J_\Gamma}$, we

introduce the mass lumped inner product $\langle \cdot, \cdot \rangle^h_{\Gamma^h(t)}$ as

$$\langle \eta, \zeta \rangle^h_{\Gamma^h(t)} := \tfrac{1}{d} \sum_{j=1}^{J_\Gamma} \mathcal{H}^{d-1}(\sigma^h_j) \sum_{k=1}^{d} (\eta \,.\, \zeta)((\vec{q}^{\,h}_{j_k})^-), \tag{3.2}$$

where $\{\vec{q}^{\,h}_{j_k}\}_{k=1}^d$ are the vertices of σ^h_j, and where we define $\eta((\vec{q}^{\,h}_{j_k})^-) := \lim_{\sigma^h_j \ni \vec{p} \to \vec{q}^{\,h}_{j_k}} \eta(\vec{p})$.

Following Dziuk and Elliott (2013, (5.23)), we define the discrete material velocity for $\vec{z} \in \Gamma^h(t)$ by

$$\vec{\mathcal{V}}^h(\vec{z}, t) := \sum_{k=1}^{K_\Gamma} \left[\frac{\mathrm{d}}{\mathrm{d}t} \vec{q}^{\,h}_k(t) \right] \chi^h_k(\vec{z}, t) \,. \tag{3.3}$$

Then, similarly to (2.19), we define

$$\partial_t^{\circ,h} \zeta = \zeta_t + \vec{\mathcal{V}}^h \,.\, \nabla \zeta \qquad \forall\ \zeta \in H^1(\mathcal{G}^h_T) \,, \tag{3.4}$$

where, similarly to (2.3), we have defined the discrete space-time surface

$$\mathcal{G}^h_T := \bigcup_{t \in [0,T]} \Gamma^h(t) \times \{t\} \,.$$

For later use, we also introduce the finite element space

$$W(\mathcal{G}^h_T) := \{ \chi \in C(\mathcal{G}^h_T) : \partial_t^{\circ,h} \chi \in C(\mathcal{G}^h_T) \text{ and } \chi(\cdot, t) \in W(\Gamma^h(t)) \quad \forall\ t \in [0,T] \} \,.$$

On differentiating (3.1) with respect to t, it immediately follows that

$$\partial_t^{\circ,h} \chi^h_k = 0 \quad \forall\ k \in \{1, \ldots, K_\Gamma\} \,, \tag{3.5}$$

see Dziuk and Elliott (2013, Lem. 5.5). It follows directly from (3.5) that

$$\partial_t^{\circ,h} \zeta(\cdot, t) = \sum_{k=1}^{K_\Gamma} \chi^h_k(\cdot, t) \frac{\mathrm{d}}{\mathrm{d}t} \zeta_k(t) \quad \text{on } \Gamma^h(t) \tag{3.6}$$

for $\zeta(\cdot, t) = \sum_{k=1}^{K_\Gamma} \zeta_k(t)\, \chi^h_k(\cdot, t) \in W(\Gamma^h(t))$, and hence $\partial_t^{\circ,h}\, \vec{\mathrm{id}} = \vec{\mathcal{V}}^h$ on $\Gamma^h(t)$. Moreover, it holds that

$$\frac{\mathrm{d}}{\mathrm{d}t} \int_{\sigma^h_j(t)} \zeta \, \mathrm{d}\mathcal{H}^{d-1} = \int_{\sigma^h_j(t)} \partial_t^{\circ,h} \zeta + \zeta \, \nabla_s \,.\, \vec{\mathcal{V}}^h \, \mathrm{d}\mathcal{H}^{d-1} \quad \forall\ \zeta \in H^1(\sigma^h_j(t)) \,, j \in \{1, \ldots, J_\Gamma\} \,, \tag{3.7}$$

see Dziuk and Elliott (2013, Lem. 5.6). It immediately follows from (3.7) that

$$\frac{\mathrm{d}}{\mathrm{d}t} \langle \eta, \zeta \rangle_{\Gamma^h(t)} = \left\langle \partial_t^{\circ,h} \eta, \zeta \right\rangle_{\Gamma^h(t)} + \left\langle \eta, \partial_t^{\circ,h} \zeta \right\rangle_{\Gamma^h(t)} + \left\langle \eta\, \zeta, \nabla_s \,.\, \vec{\mathcal{V}}^h \right\rangle_{\Gamma^h(t)} \qquad \forall\ \eta, \zeta \in W(\mathcal{G}^h_T) \,, \tag{3.8}$$

which is a discrete analogue of (2.21). It is not difficult to show that the analogue of (3.8) with numerical integration also holds. We establish this result in the next lemma, together with a discrete variant of (2.22), on recalling (2.8), for the case $d = 2$.

LEMMA. 3.1. *It holds that*

$$\frac{\mathrm{d}}{\mathrm{d}t}\,\langle \eta,\zeta\rangle^h_{\Gamma^h(t)} = \Big\langle \partial_t^{\circ,h}\,\eta,\zeta\Big\rangle^h_{\Gamma^h(t)} + \Big\langle \eta,\partial_t^{\circ,h}\,\zeta\Big\rangle^h_{\Gamma^h(t)} + \Big\langle \eta\,\zeta,\nabla_s\,.\,\vec{\mathcal{V}}^h\Big\rangle^h_{\Gamma^h(t)} \quad \forall\ \eta,\zeta\in W(\mathcal{G}^h_T)\,. \tag{3.9}$$

In addition, if $d=2$, it holds that

$$\langle \zeta,\nabla_s\,.\,\vec{\eta}\rangle_{\Gamma^h(t)} + \langle \nabla_s\,\zeta,\vec{\eta}\rangle_{\Gamma^h(t)} = \Big\langle \nabla_s\,\vec{\mathrm{id}},\nabla_s\,\vec{\pi}^h\,(\zeta\,\vec{\eta})\Big\rangle_{\Gamma^h(t)} \quad \forall\ \zeta\in W(\Gamma^h(t))\,,\vec{\eta}\in \underline{V}(\Gamma^h(t))\,. \tag{3.10}$$

Proof. Choosing $\zeta=1$ in (3.7) yields that

$$\frac{\mathrm{d}}{\mathrm{d}t}\,\mathcal{H}^{d-1}(\sigma^h_j(t)) = \mathcal{H}^{d-1}(\sigma^h_j(t))\,\nabla_s\,.\,\vec{\mathcal{V}}^h(\cdot,t) \quad \text{on } \sigma^h_j(t)\,. \tag{3.11}$$

Differentiating (3.2) with respect to t, and combining with (3.11) and (3.6), yields the desired result (3.9).

For arbitrary $\zeta\in H^1(\Gamma^h(t))$ and $\vec{\eta}\in[H^1(\Gamma^h(t))]^2$ we have for $d=2$ that

$$\langle \nabla_s\,.\,(\zeta\,\vec{\eta}),1\rangle_{\Gamma^h(t)} = \Big\langle \vec{\mathrm{id}}_s,(\zeta\,\vec{\eta})_s\Big\rangle_{\Gamma^h(t)} = \Big\langle \vec{\mathrm{id}}_s,(\vec{\pi}^h\,[\zeta\,\vec{\eta}])_s\Big\rangle_{\Gamma^h(t)} = \Big\langle \nabla_s\,\vec{\mathrm{id}},\nabla_s\,\vec{\pi}^h\,(\zeta\,\vec{\eta})\Big\rangle_{\Gamma^h(t)}\,,$$

which yields the desired result (3.10) on noting that $\nabla_s\,.\,(\zeta\,\vec{\eta}) = \zeta\,\nabla_s\,.\,\vec{\eta} + \vec{\eta}\,.\,\nabla_s\,\zeta$. ∎

Given $\Gamma^h(t)$, we let $\Omega^h_+(t)$ denote the exterior of $\Gamma^h(t)$ and let $\Omega^h_-(t)$ denote the interior of $\Gamma^h(t)$, so that $\Gamma^h(t)=\partial\Omega^h_-(t)=\overline{\Omega^h_-(t)}\cap\overline{\Omega^h_+(t)}$. We then partition the elements of the bulk mesh $\mathcal{T}^h$ into interior, exterior and interfacial elements as follows. Let

$$\begin{aligned}
\mathcal{T}^h_-(t) &:= \{o\in\mathcal{T}^h : o\subset\Omega^h_-(t)\}\,,\\
\mathcal{T}^h_+(t) &:= \{o\in\mathcal{T}^h : o\subset\Omega^h_+(t)\}\,,\\
\mathcal{T}^h_{\Gamma^h}(t) &:= \{o\in\mathcal{T}^h : o\cap\Gamma^h(t)\neq\emptyset\}\,.
\end{aligned}$$

Clearly $\mathcal{T}^h=\mathcal{T}^h_-(t)\cup\mathcal{T}^h_+(t)\cup\mathcal{T}^h_\Gamma(t)$ is a disjoint partition. In addition, we define the piecewise constant unit normal $\vec{\nu}^h(t)$ to $\Gamma^h(t)$ such that $\vec{\nu}^h(t)$ points into $\Omega^h_+(t)$. Moreover, we introduce the discrete density $\rho^h(t)\in S^h_0$ and the discrete viscosity $\mu^h(t)\in S^h_0$ as

$$\rho^h(t)\,|_o = \begin{cases} \rho_- & o\in\mathcal{T}^h_-(t)\,,\\ \rho_+ & o\in\mathcal{T}^h_+(t)\,,\\ \frac12\,(\rho_-+\rho_+) & o\in\mathcal{T}^h_{\Gamma^h}(t)\,,\end{cases} \quad\text{and}\quad \mu^h(t)\,|_o = \begin{cases} \mu_- & o\in\mathcal{T}^h_-(t)\,,\\ \mu_+ & o\in\mathcal{T}^h_+(t)\,,\\ \frac12\,(\mu_-+\mu_+) & o\in\mathcal{T}^h_{\Gamma^h}(t)\,.\end{cases}$$

In what follows we will introduce two different finite element approximations for the free boundary problem (2.4a–d), (2.5), (2.6a–c), (2.9). Here $\vec{U}^h(\cdot,t)\in\mathbb{U}^h$ will be an approximation to $\vec{u}(\cdot,t)$, while $P^h(\cdot,t)\in\widehat{\mathbb{P}}^h(t)$ approximates $p(\cdot,t)$ and $\Psi^h(\cdot,t)\in W(\Gamma^h(t))$ approximates $\psi(\cdot,t)$. When designing such a finite element approximation, a careful decision has to be made about the *discrete tangential velocity* of $\Gamma^h(t)$. The most natural choice

is to select the velocity of the fluid, i.e. (2.24c) is appropriately discretized. This then gives a natural discretization of the surfactant transport equation (2.9). Note also that the approximation of curvature, recall (2.8), where now $\vec{\varkappa} = \varkappa\,\vec{\nu}$ is discretized directly, goes back to the seminal paper Dziuk (1991). Overall, we then obtain the following semidiscrete continuous-in-time finite element approximation, which is the semidiscrete analogue of the weak formulation (2.24a–e). Given $\Gamma^h(0)$, $\vec{U}^h(\cdot,0) \in \mathbb{U}^h$ and $\Psi^h(\cdot,0) \in W(\Gamma^h(0))$, find $\Gamma^h(t)$ such that $\vec{\mathrm{id}}\,|_{\Gamma^h(t)} \in \underline{V}(\Gamma^h(t))$ for $t \in [0,T]$, and functions $\vec{U}^h \in H^1(0,T;\mathbb{U}^h)$, $P^h \in L^2(0,T;\widehat{\mathbb{P}}^h(t))$, $\vec{\kappa}^h \in L^2(0,T;\underline{V}(\Gamma^h(t)))$ and $\Psi^h \in W(\mathcal{G}_T^h)$ such that for almost all $t \in (0,T)$ it holds that

$$\begin{aligned}
&\tfrac{1}{2}\left[\frac{\mathrm{d}}{\mathrm{d}t}\left(\rho^h\,\vec{U}^h,\vec{\xi}\right) + \left(\rho^h\,\vec{U}^h_t,\vec{\xi}\right) - \left(\rho^h\,\vec{U}^h,\vec{\xi}_t\right)\right] \\
&\qquad + 2\left(\mu^h\,\underline{\underline{D}}(\vec{U}^h),\underline{\underline{D}}(\vec{\xi})\right) + \tfrac{1}{2}\left(\rho^h,[(\vec{I}_2^h\,\vec{U}^h\,.\,\nabla)\,\vec{U}^h]\,.\,\vec{\xi} - [(\vec{I}_2^h\,\vec{U}^h\,.\,\nabla)\,\vec{\xi}]\,.\,\vec{U}^h\right) \\
&\qquad - \left(P^h,\nabla\,.\,\vec{\xi}\right) = \left(\rho^h\,\vec{f}_1^h + \vec{f}_2^h,\vec{\xi}\right) + \left\langle \gamma(\Psi^h)\,\vec{\kappa}^h + \nabla_s\,\pi^h\,[\gamma(\Psi^h)],\vec{\xi}\right\rangle^h_{\Gamma^h(t)} \\
&\qquad\qquad \forall\ \vec{\xi} \in H^1(0,T;\mathbb{U}^h)\,, \qquad \text{(3.12a)}
\end{aligned}$$

$$\left(\nabla\,.\,\vec{U}^h,\varphi\right) = 0 \qquad \forall\ \varphi \in \widehat{\mathbb{P}}^h(t)\,, \qquad \text{(3.12b)}$$

$$\left\langle \vec{\mathcal{V}}^h,\vec{\chi}\right\rangle^h_{\Gamma^h(t)} = \left\langle \vec{U}^h,\vec{\chi}\right\rangle^h_{\Gamma^h(t)} \qquad \forall\ \vec{\chi} \in \underline{V}(\Gamma^h(t))\,, \qquad \text{(3.12c)}$$

$$\left\langle \vec{\kappa}^h,\vec{\eta}\right\rangle^h_{\Gamma^h(t)} + \left\langle \nabla_s\,\vec{\mathrm{id}},\nabla_s\,\vec{\eta}\right\rangle_{\Gamma^h(t)} = 0 \qquad \forall\ \vec{\eta} \in \underline{V}(\Gamma^h(t))\,, \qquad \text{(3.12d)}$$

$$\frac{\mathrm{d}}{\mathrm{d}t}\left\langle \Psi^h,\chi\right\rangle^h_{\Gamma^h(t)} + \mathcal{D}_\Gamma\left\langle \nabla_s\,\Psi^h,\nabla_s\,\chi\right\rangle_{\Gamma^h(t)} = \left\langle \Psi^h,\partial_t^{\circ,h}\,\chi\right\rangle^h_{\Gamma^h(t)} \qquad \forall\ \chi \in W(\mathcal{G}_T^h)\,, \qquad \text{(3.12e)}$$

where we recall (3.3). Here we have defined $\vec{f}_i^h(\cdot,t) := \vec{I}_2^h\,\vec{f}_i(\cdot,t)$, $i = 1,2$, where here and throughout we assume that $\vec{f}_i \in L^2(0,T;[C(\overline{\Omega})]^d)$, $i = 1,2$. We observe that (3.12c) collapses to $\vec{\mathcal{V}}^h = \vec{\pi}^h\,\vec{U}^h\,|_{\Gamma^h(t)} \in \underline{V}(\Gamma^h(t))$, which on recalling (3.4) turns out to be crucial for the stability analysis for (3.12a–e). It is for this reason that we use mass lumping in (3.12c), which then leads to mass lumping having to be used in the last term in (3.12a), as well as for the first term in (3.12d).

We remark that the formulation (3.12e) for the surfactant transport equation (2.9) falls into the framework of ESFEM (evolving surface finite element method) as coined by the authors in Dziuk and Elliott (2007). In this particular instance, the velocity of $\Gamma^h(t)$ is not a priori fixed, rather it arises implicitly through the evolution of $\Gamma^h(t)$ as determined by (3.12a–e). Here we recall the important property (3.5), which means that (3.12e) simplifies if formulated in terms of the basis functions $\{\chi_k^h(\cdot,t)\}_{k=1}^{K_\Gamma}$ of $W(\Gamma^h(t))$.

In the following lemma we derive a discrete analogue of (2.25).

LEMMA. 3.2. *Let* $\{(\Gamma^h, \vec{U}^h, P^h, \vec{\kappa}^h, \Psi^h)(t)\}_{t\in[0,T]}$ *be a solution to* (3.12a–e). *Then*

$$\begin{aligned}\tfrac{1}{2}\,\frac{\mathrm{d}}{\mathrm{d}t}\,\|[\rho^h]^{\frac{1}{2}}\,\vec{U}^h\|_0^2 + 2\,\|[\mu^h]^{\frac{1}{2}}\,\underline{\underline{D}}(\vec{U}^h)\|_0^2 \\ = (\rho^h\,\vec{f}_1^{\,h} + \vec{f}_2^{\,h}, \vec{U}^h) + \Big\langle \gamma(\Psi^h)\,\vec{\kappa}^h + \nabla_s\,\pi^h\,[\gamma(\Psi^h)], \vec{U}^h \Big\rangle_{\Gamma^h(t)}^h\,. \end{aligned} \tag{3.13}$$

Proof. The desired result (3.13) follows immediately on choosing $\vec{\xi} = \vec{U}^h$ in (3.12a) and $\varphi = P^h$ in (3.12b). □

The next theorem derives a discrete analogue of the energy law (2.31). Here, similarly to (2.26), it will be crucial to test (3.12e) with an appropriate discrete variant of $F'(\Psi^h)$. It is for this reason that we have to make the following well-posedness assumption.

$$\Psi^h(\cdot,t) < \psi_\infty \quad \text{on } \Gamma^h(t)\,, \quad \forall\, t\in[0,T]\,. \tag{3.14}$$

The theorem also establishes nonnegativity of Ψ^h under the assumption that

$$\int_{\sigma_j^h(t)} \nabla_s\chi_i^h\,.\,\nabla_s\chi_k^h\,\mathrm{d}\mathcal{H}^{d-1} \le 0 \quad \forall\, i\neq k\,, \quad \forall\, t\in[0,T]\,, \qquad j=1,\ldots,J_\Gamma\,. \tag{3.15}$$

We note that (3.15) always holds for $d=2$, and it holds for $d=3$ if all the triangles $\sigma_j^h(t)$ of $\Gamma^h(t)$ have no obtuse angles. A direct consequence of (3.15) is that for any monotonic function $G\in C^{0,1}(\mathbb{R})$ it holds that

$$\begin{aligned} L_G\,\big\langle \nabla_s\,\xi, \nabla_s\,\pi^h\,[G(\xi)]\big\rangle_{\Gamma^h(t)} \ge \big\langle \nabla_s\,\pi^h\,[G(\xi)], \nabla_s\,\pi^h\,[G(\xi)]\big\rangle_{\Gamma^h(t)} \quad \forall\,\xi\in W(\Gamma^h(t))\,, \\ \forall\, t\in[0,T]\,, \end{aligned} \tag{3.16}$$

where $L_G\in\mathbb{R}_{>0}$ denotes its Lipschitz constant. For example, (3.16) holds for $G(r) = [r]_- := \min\{0,r\}$ with $L_G = 1$.

For the following theorem, we denote the L^∞–norm on $\Gamma^h(t)$ by $\|\cdot\|_{\infty,\Gamma^h(t)}$, i.e. $\|z\|_{\infty,\Gamma^h(t)} := \operatorname{ess\,sup}_{\Gamma^h(t)}|z|$ for $z:\Gamma^h(t)\to\mathbb{R}$.

THEOREM. 3.3. *Let* $\{(\Gamma^h, \vec{U}^h, P^h, \vec{\kappa}^h, \Psi^h)(t)\}_{t\in[0,T]}$ *be a solution to* (3.12a–e). *Then*

$$\frac{\mathrm{d}}{\mathrm{d}t}\,\big\langle \Psi^h, 1\big\rangle_{\Gamma^h(t)} = 0\,. \tag{3.17}$$

In addition, if $\mathcal{D}_\Gamma = 0$ *or if* (3.15) *and*

$$\max_{0\le t\le T}\|\nabla_s\,.\,\vec{\mathcal{V}}^h\|_{\infty,\Gamma^h(t)} < \infty \tag{3.18}$$

hold, then

$$\Psi^h(\cdot,t)\ge 0 \quad \forall\, t\in(0,T] \qquad \text{if} \quad \Psi^h(\cdot,0)\ge 0\,. \tag{3.19}$$

Moreover, if $d=2$ *and if* (3.19) *and* (3.14) *hold, then*

$$\frac{\mathrm{d}}{\mathrm{d}t}\left(\tfrac{1}{2}\,\|[\rho^h]^{\frac{1}{2}}\,\vec{U}^h\|_0^2 + \big\langle F(\Psi^h),1\big\rangle_{\Gamma^h(t)}^h\right) + 2\,\|[\mu^h]^{\frac{1}{2}}\,\underline{\underline{D}}(\vec{U}^h)\|_0^2 \le \left(\rho^h\,\vec{f}_1^{\,h} + \vec{f}_2^{\,h}, \vec{U}^h\right). \tag{3.20}$$

Proof. The conservation property (3.17) follows immediately from choosing $\chi = 1$ in (3.12e).

If $\mathcal{D}_\Gamma = 0$ then it immediately follows from (3.12e), on recalling (3.5), that

$$\frac{\mathrm{d}}{\mathrm{d}t} \left\langle \Psi^h, \chi^h_k \right\rangle^h_{\Gamma^h(t)} = \frac{\mathrm{d}}{\mathrm{d}t} \left[\left\langle 1, \chi^h_k \right\rangle_{\Gamma^h(t)} \Psi^h(\vec{q}^h_k(t), t) \right] = 0 \,,$$

for $k = 1, \ldots, K_\Gamma$, which yields the desired result (3.19) if $\mathcal{D}_\Gamma = 0$. If $\mathcal{D}_\Gamma > 0$, then choosing $\chi = \pi^h [\Psi^h]_-$ in (3.12e) yields, on noting (3.16) with $G = [\cdot]_-$ and (3.9), that

$$\begin{aligned}
\frac{\mathrm{d}}{\mathrm{d}t} \left\langle [\Psi^h]^2_-, 1 \right\rangle^h_{\Gamma^h(t)} &= \frac{\mathrm{d}}{\mathrm{d}t} \left\langle \Psi^h, [\Psi^h]_- \right\rangle^h_{\Gamma^h(t)} \leq \left\langle \Psi^h, \partial_t^{\circ,h} \pi^h [\Psi^h]_- \right\rangle^h_{\Gamma^h(t)} \\
&= \left\langle [\Psi^h]_-, \partial_t^{\circ,h} \pi^h [\Psi^h]_- \right\rangle^h_{\Gamma^h(t)} = \tfrac{1}{2} \left\langle \partial_t^{\circ,h} \pi^h [\Psi^h]^2_-, 1 \right\rangle^h_{\Gamma^h(t)} \\
&= \tfrac{1}{2} \frac{\mathrm{d}}{\mathrm{d}t} \left\langle \pi^h [\Psi^h]^2_-, 1 \right\rangle^h_{\Gamma^h(t)} - \tfrac{1}{2} \left\langle \pi^h [\Psi^h]^2_-, \nabla_s \,.\, \vec{\mathcal{V}}^h \right\rangle^h_{\Gamma^h(t)} \\
&\leq - \left\langle \pi^h [\Psi^h]^2_-, \nabla_s \,.\, \vec{\mathcal{V}}^h \right\rangle^h_{\Gamma^h(t)} \leq \| \nabla_s \,.\, \vec{\mathcal{V}}^h \|_{\infty,\Gamma^h(t)} \left\langle \pi^h [\Psi^h]^2_-, 1 \right\rangle^h_{\Gamma^h(t)} \,.
\end{aligned}$$

A Gronwall inequality, together with (3.18), now yields our desired result (3.19).

For the proof of (3.20) we note that the assumption (3.14) means that we can choose $\chi = \pi^h [F'(\Psi^h + \alpha)]$ in (3.12e), with $\alpha \in \mathbb{R}_{>0}$ such that $\Psi^h + \alpha < \psi_\infty$, to yield, on recalling (2.12a) and (3.9), that

$$\begin{aligned}
&\frac{\mathrm{d}}{\mathrm{d}t} \left\langle F(\Psi^h + \alpha) - \gamma(\Psi^h + \alpha), 1 \right\rangle^h_{\Gamma^h(t)} + \mathcal{D}_\Gamma \left\langle \nabla_s (\Psi^h + \alpha), \nabla_s \pi^h [F'(\Psi^h + \alpha)] \right\rangle_{\Gamma^h(t)} \\
&\quad = \left\langle \Psi^h + \alpha, \partial_t^{\circ,h} \pi^h [F'(\Psi^h + \alpha)] \right\rangle^h_{\Gamma^h(t)} + \alpha \left\langle F'(\Psi^h + \alpha), \nabla_s \,.\, \vec{\mathcal{V}}^h \right\rangle^h_{\Gamma^h(t)} \,, \qquad (3.21)
\end{aligned}$$

similarly to (2.26). For the remainder of the proof we assume that $d = 2$. It follows from (2.13), (3.2) and (3.6) that we have a discrete analogue of (2.28), i.e.

$$\left\langle \Psi^h + \alpha, \partial_t^{\circ,h} \pi^h [F'(\Psi^h + \alpha)] \right\rangle^h_{\Gamma^h(t)} = - \left\langle \partial_t^{\circ,h} \pi^h [\gamma(\Psi^h + \alpha)], 1 \right\rangle^h_{\Gamma^h(t)} \,, \qquad (3.22)$$

which means that (3.21), together with (3.9), (3.10) and (3.12c,d), implies that

$$\begin{aligned}
&\frac{\mathrm{d}}{\mathrm{d}t} \left\langle F(\Psi^h + \alpha), 1 \right\rangle^h_{\Gamma^h(t)} + \mathcal{D}_\Gamma \left\langle \nabla_s (\Psi^h + \alpha), \nabla_s \pi^h [F'(\Psi^h + \alpha)] \right\rangle_{\Gamma^h(t)} \\
&\quad = \left\langle \pi^h [\gamma(\Psi^h + \alpha)], \nabla_s \,.\, \vec{\mathcal{V}}^h \right\rangle_{\Gamma^h(t)} + \alpha \left\langle F'(\Psi^h + \alpha), \nabla_s \,.\, \vec{\mathcal{V}}^h \right\rangle^h_{\Gamma^h(t)} \\
&\quad = \left\langle \nabla_s \vec{\mathrm{id}}, \nabla_s \pi^h [\gamma(\Psi^h + \alpha) \vec{\mathcal{V}}^h] \right\rangle_{\Gamma^h(t)} - \left\langle \nabla_s \pi^h [\gamma(\Psi^h + \alpha)], \vec{\mathcal{V}}^h \right\rangle_{\Gamma^h(t)} \\
&\qquad + \alpha \left\langle F'(\Psi^h + \alpha), \nabla_s \,.\, \vec{\mathcal{V}}^h \right\rangle^h_{\Gamma^h(t)} \\
&\quad = - \left\langle \vec{\kappa}^h, \gamma(\Psi^h + \alpha) \vec{U}^h \right\rangle^h_{\Gamma^h(t)} - \left\langle \nabla_s \pi^h [\gamma(\Psi^h + \alpha)], \vec{U}^h \right\rangle^h_{\Gamma^h(t)} \\
&\qquad + \alpha \left\langle F'(\Psi^h + \alpha), \nabla_s \,.\, \vec{\mathcal{V}}^h \right\rangle^h_{\Gamma^h(t)} \,. \qquad (3.23)
\end{aligned}$$

Next, on noting for $\mathcal{D}_\Gamma > 0$ that $G(\cdot) = F'(\cdot + \alpha)$ is monotonic, as F is convex, and has a finite Lipschitz constant, on noting (3.19), it follows from our assumptions and (3.16) that

$$\mathcal{D}_\Gamma \left\langle \nabla_s \left(\Psi^h + \alpha\right), \nabla_s \, \pi^h \left[F'(\Psi^h + \alpha)\right] \right\rangle_{\Gamma^h(t)} \geq 0 \,, \tag{3.24}$$

and so we obtain that

$$\begin{aligned} \frac{\mathrm{d}}{\mathrm{d}t} \left\langle F(\Psi^h + \alpha), 1 \right\rangle^h_{\Gamma^h(t)} \leq & - \left\langle \vec{\kappa}^h, \gamma(\Psi^h + \alpha) \, \vec{U}^h \right\rangle^h_{\Gamma^h(t)} - \left\langle \nabla_s \, \pi^h \left[\gamma(\Psi^h + \alpha)\right], \vec{U}^h \right\rangle^h_{\Gamma^h(t)} \\ & + \alpha \left\langle F'(\Psi^h + \alpha), \nabla_s \,.\, \vec{\mathcal{V}}^h \right\rangle^h_{\Gamma^h(t)} \,. \end{aligned} \tag{3.25}$$

Passing to the limit $\alpha \to 0$ in (3.25), noting (2.12b), and combining with (3.13), yields the desired result (3.20). □

Clearly, (3.17) and (3.20) are natural discrete analogues of (2.33) and (2.31), respectively.

We note that while (3.12a–e) is a very natural approximation, in particular (3.12e) for the surfactant transport, see also Dziuk and Elliott (2007), a drawback in practice is that the finitely many vertices of the triangulations $\Gamma^h(t)$ are moved with the flow, which can lead to coalescence. If a remeshing procedure is applied to $\Gamma^h(t)$, then theoretical results like stability are no longer valid.

It is with this in mind that we would like to introduce an alternative finite element approximation. It will be based on the weak formulation (2.35a–e), and on the schemes from Barrett *et al.* (2013a,b) for the two-phase flow problem in the bulk. Of course, the discretization of (2.35e) is going to be more complicated than (3.12e), but the advantage is that good mesh properties can be shown for $\Gamma^h(t)$. In practice this means that no remeshings or reparameterizations need to be performed for $\Gamma^h(t)$.

The main difference to (3.12a–e) is that (3.12c) is replaced with a discrete variant of (2.35c). In particular, the discrete tangential velocity of $\Gamma^h(t)$ is not defined via $\vec{U}^h(\cdot, t)$, but it is chosen totally independent from the surrounding fluid. In fact, the discrete tangential velocity is not prescribed directly, but it is implicitly introduced via the novel approximation of curvature which was first introduced by the authors in Barrett *et al.* (2007) for the case $d = 2$, and in Barrett *et al.* (2008) for the case $d = 3$. This discrete tangential velocity is such that, in the case $d = 2$, $\Gamma^h(t)$ will remain equidistributed for all times $t \in (0, T]$. For $d = 3$, a weaker property can be shown, which still guarantees good meshes in practice. We refer to Barrett *et al.* (2007, 2008) for more details.

For this new finite element approximation we are unable to guarantee the nonnegativity of $\Psi^h(\cdot, t)$, which is in contrast to the result (3.19) for the scheme (3.12a–e). It is for this reason that, following similar ideas in Barrett *et al.* (2003); Barrett and Nürnberg (2004), we introduce regularizations $F_\varepsilon \in C^2(-\infty, \psi_\infty)$ of $F \in C^2(0, \psi_\infty)$, where $\varepsilon > 0$ is a regularization parameter. In particular, we set

$$F_\varepsilon(r) = \begin{cases} F(r) & r \geq \varepsilon \,, \\ F(\varepsilon) + F'(\varepsilon) \, (r - \varepsilon) + \frac{1}{2} \, F''(\varepsilon) \, (r - \varepsilon)^2 & r \leq \varepsilon \,, \end{cases} \tag{3.26a}$$

which in view of (2.12a) leads to

$$\gamma_\varepsilon(r) = \begin{cases} \gamma(r) & r \geq \varepsilon\,, \\ \gamma(\varepsilon) + \frac{1}{2}\,F''(\varepsilon)\,(\varepsilon^2 - r^2) & r \leq \varepsilon\,, \end{cases} \tag{3.26b}$$

so that

$$\gamma_\varepsilon(r) = F_\varepsilon(r) - r\,F'_\varepsilon(r) \quad \text{and} \quad \gamma'_\varepsilon(r) = -r\,F''_\varepsilon(r) \qquad \forall\ r < \psi_\infty\,. \tag{3.27}$$

We propose the following semidiscrete continuous-in-time finite element approximation, which is the semidiscrete analogue of the weak formulation (2.35a–e). Given $\Gamma^h(0)$, $\vec{U}^h(\cdot,0) \in \mathbb{U}^h$ and $\Psi^h(\cdot,0) \in W(\Gamma^h(0))$, find $\Gamma^h(t)$ such that $\vec{\mathrm{id}}\,|_{\Gamma^h(t)} \in \underline{V}(\Gamma^h(t))$ for $t \in [0,T]$, and functions $\vec{U}^h \in H^1(0,T;\mathbb{U}^h)$, $P^h \in L^2(0,T;\widehat{\mathbb{P}}^h(t))$, $\kappa^h \in L^2(0,T;W(\Gamma^h(t)))$ and $\Psi^h \in W(\mathcal{G}^h_T)$ such that for almost all $t \in (0,T)$ it holds that

$$\begin{aligned} &\tfrac{1}{2}\left[\frac{\mathrm{d}}{\mathrm{d}t}\left(\rho^h\,\vec{U}^h, \vec{\xi}\right) + \left(\rho^h\,\vec{U}^h_t, \vec{\xi}\right) - \left(\rho^h\,\vec{U}^h, \vec{\xi}_t\right)\right] \\ &\quad + 2\left(\mu^h\,\underline{\underline{D}}(\vec{U}^h), \underline{\underline{D}}(\vec{\xi})\right) + \tfrac{1}{2}\left(\rho^h, [(\vec{I}^h_2\,\vec{U}^h\,.\,\nabla)\,\vec{U}^h]\,.\,\vec{\xi} - [(\vec{I}^h_2\,\vec{U}^h\,.\,\nabla)\,\vec{\xi}]\,.\,\vec{U}^h\right) \\ &\quad - \left(P^h, \nabla\,.\,\vec{\xi}\right) = \left(\rho^h\,\vec{f}^h_1 + \vec{f}^h_2, \vec{\xi}\right) + \left\langle \pi^h\,[\gamma_\varepsilon(\Psi^h)\,\kappa^h]\,\vec{\nu}^h, \vec{\xi}\right\rangle_{\Gamma^h(t)} \\ &\qquad\qquad + \left\langle \nabla_s\,\pi^h\,[\gamma_\varepsilon(\Psi^h)], \vec{\xi}\right\rangle^h_{\Gamma^h(t)} \qquad \forall\ \vec{\xi} \in H^1(0,T;\mathbb{U}^h)\,, \end{aligned} \tag{3.28a}$$

$$\left(\nabla\,.\,\vec{U}^h, \varphi\right) = 0 \quad \forall\ \varphi \in \widehat{\mathbb{P}}^h(t)\,, \tag{3.28b}$$

$$\left\langle \vec{\mathcal{V}}^h, \chi\,\vec{\nu}^h\right\rangle^h_{\Gamma^h(t)} = \left\langle \vec{U}^h, \chi\,\vec{\nu}^h\right\rangle_{\Gamma^h(t)} \qquad \forall\ \chi \in W(\Gamma^h(t))\,, \tag{3.28c}$$

$$\left\langle \kappa^h\,\vec{\nu}^h, \vec{\eta}\right\rangle^h_{\Gamma^h(t)} + \left\langle \nabla_s\,\vec{\mathrm{id}}, \nabla_s\,\vec{\eta}\right\rangle_{\Gamma^h(t)} = 0 \quad \forall\ \vec{\eta} \in \underline{V}(\Gamma^h(t))\,, \tag{3.28d}$$

$$\begin{aligned} &\frac{\mathrm{d}}{\mathrm{d}t}\left\langle \Psi^h, \chi\right\rangle^h_{\Gamma^h(t)} + \mathcal{D}_\Gamma\left\langle \nabla_s\,\Psi^h, \nabla_s\,\chi\right\rangle_{\Gamma^h(t)} = \left\langle \Psi^h, \partial_t^{\circ,h}\,\chi\right\rangle^h_{\Gamma^h(t)} - \left\langle \Psi^h_{\star,\varepsilon}\left(\vec{\mathcal{V}}^h - \vec{U}^h\right), \nabla_s\,\chi\right\rangle^h_{\Gamma^h(t)} \\ &\qquad\qquad \forall\ \chi \in W(\mathcal{G}^h_T)\,, \end{aligned} \tag{3.28e}$$

where we recall (3.3). Here $\Psi^h_{\star,\varepsilon} = \Psi^h$ for $d = 3$ and, on recalling (3.27),

$$\Psi^h_{\star,\varepsilon} = \begin{cases} -\frac{\gamma_\varepsilon(\Psi^h_k) - \gamma_\varepsilon(\Psi^h_{k-1})}{F'_\varepsilon(\Psi^h_k) - F'_\varepsilon(\Psi^h_{k-1})} & F'_\varepsilon(\Psi^h_{k-1}) \neq F'_\varepsilon(\Psi^h_k)\,, \\ \frac{1}{2}\,(\Psi^h_{k-1} + \Psi^h_k) & F'_\varepsilon(\Psi^h_{k-1}) = F'_\varepsilon(\Psi^h_k)\,, \end{cases} \quad \text{on} \quad [\vec{q}^h_{k-1}, \vec{q}^h_k] \quad \forall\ k \in \{1,\ldots,K_\Gamma\} \tag{3.29}$$

for $d = 2$. Here we have introduced the shorthand notation $\Psi^h_k(t) = \Psi^h(\vec{q}^h_k(t), t)$, for $k = 1,\ldots,K_\Gamma$, and for notational convenience we have dropped the dependence on t in (3.29). The definition in (3.29) is chosen such that for $d = 2$ it holds that

$$\left\langle \Psi^h_{\star,\varepsilon}\,\vec{\eta}, \nabla_s\,\pi^h\,[F'_\varepsilon(\Psi^h)]\right\rangle^h_{\Gamma^h(t)} = \left\langle \Psi^h_{\star,\varepsilon}\,\vec{\eta}, \nabla_s\,\pi^h\,[F'_\varepsilon(\Psi^h)]\right\rangle_{\Gamma^h(t)} = -\left\langle \vec{\eta}, \nabla_s\,\pi^h\,[\gamma_\varepsilon(\Psi^h)]\right\rangle_{\Gamma^h(t)} \qquad \forall\ \vec{\eta} \in \underline{V}(\Gamma^h(t))\,, \tag{3.30}$$

which will be crucial for the stability proof for (3.28a–e). Note that here the regularization (3.26a,b) is required in order to make the definition (3.29) well-defined, where we recall from (2.12a) that F' in general is only well-defined on the positive real line. We observe that (3.30) for $\vec{\eta} = \vec{\mathcal{V}}^h - \vec{\pi}^h \, \vec{U}^h|_{\Gamma^h(t)}$ mimics (2.36) on the discrete level.

Similarly to Theorem 3.3 we are only able to prove stability for the scheme (3.28a–e) in the case $d = 2$. Hence in the case $d = 3$ the definition (3.29) is not required, and so γ_ε in (3.28a) may also be replaced by γ.

We remark that the formulation (3.28e) for the surfactant transport equation (2.9) falls into the framework of ALE ESFEM (arbitrary Lagrangian Eulerian evolving surface finite element method) as coined by the authors in Elliott and Styles (2012). In this particular instance, the tangential velocity of $\Gamma^h(t)$ is not a priori fixed, rather it arises implicitly through the evolution of $\Gamma^h(t)$ as determined by (3.28a–e).

Similarly to Lemma 3.2, in the following lemma we derive a discrete analogue of (2.25).

LEMMA. 3.4. *Let* $\{(\Gamma^h, \vec{U}^h, P^h, \kappa^h, \Psi^h)(t)\}_{t\in[0,T]}$ *be a solution to* (3.28a–e). *Then*

$$\begin{aligned}
&\tfrac{1}{2}\,\frac{\mathrm{d}}{\mathrm{d}t}\,\|[\rho^h]^{\frac12}\,\vec{U}^h\|_0^2 + 2\,\|[\mu^h]^{\frac12}\,\underline{\underline{D}}(\vec{U}^h)\|_0^2 \\
&\qquad = (\rho^h\,\vec{f}_1^{\,h} + \vec{f}_2^{\,h}, \vec{U}^h) + \left\langle \pi^h\,[\gamma_\varepsilon(\Psi^h)\,\kappa^h]\,\vec{\nu}^h, \vec{U}^h \right\rangle_{\Gamma^h(t)} + \left\langle \nabla_s\,\pi^h\,[\gamma_\varepsilon(\Psi^h)], \vec{U}^h \right\rangle^h_{\Gamma^h(t)} .
\end{aligned} \tag{3.31}$$

Proof. The desired result (3.31) follows immediately on choosing $\vec{\xi} = \vec{U}^h$ in (3.28a) and $\varphi = P^h$ in (3.28b). □

The next theorem derives a discrete analogue of the energy law (2.31), similarly to Theorem 3.3, together with an exact volume conservation property.

THEOREM. 3.5. *Let* $\{(\Gamma^h, \vec{U}^h, P^h, \kappa^h, \Psi^h)(t)\}_{t\in[0,T]}$ *be a solution to* (3.28a–e). *Then*

$$\frac{\mathrm{d}}{\mathrm{d}t}\,\left\langle \Psi^h, 1 \right\rangle_{\Gamma^h(t)} = 0\,. \tag{3.32}$$

Moreover, if $\mathcal{X}_{\Omega^h_-(t)} \in \mathbb{P}^h(t)$ *then*

$$\frac{\mathrm{d}}{\mathrm{d}t}\,\mathcal{L}^d(\Omega^h_-(t)) = 0\,. \tag{3.33}$$

In addition, if $d = 2$ *and if the assumption* (3.14) *holds, then*

$$\frac{\mathrm{d}}{\mathrm{d}t}\left(\tfrac{1}{2}\,\|[\rho^h]^{\frac12}\,\vec{U}^h\|_0^2 + \left\langle F_\varepsilon(\Psi^h), 1\right\rangle^h_{\Gamma^h(t)}\right) + 2\,\|[\mu^h]^{\frac12}\,\underline{\underline{D}}(\vec{U}^h)\|_0^2 \leq \left(\rho^h\,\vec{f}_1^{\,h} + \vec{f}_2^{\,h}, \vec{U}^h\right). \tag{3.34}$$

Proof. The conservation property (3.32) follows immediately from choosing $\chi = 1$ in (3.28e). Moreover, choosing $\chi = 1$ in (3.28c) and $\varphi = (\mathcal{X}_{\Omega^h_-(t)} - \frac{\mathcal{L}^d(\Omega^h_-(t))}{\mathcal{L}^d(\Omega)}) \in \widehat{\mathbb{P}}^h(t)$ in

(3.28b), we obtain that

$$\frac{\mathrm{d}}{\mathrm{d}t}\mathcal{L}^d(\Omega^h_-(t)) = \left\langle \vec{\mathcal{V}}^h, \vec{\nu}^h \right\rangle_{\Gamma^h(t)} = \left\langle \vec{\mathcal{V}}^h, \vec{\nu}^h \right\rangle^h_{\Gamma^h(t)} = \left\langle \vec{U}^h, \vec{\nu}^h \right\rangle_{\Gamma^h(t)} = \int_{\Omega^h_-(t)} \nabla \,.\, \vec{U}^h \,\mathrm{d}\mathcal{L}^d = 0\,,$$

which proves the desired result (3.33). For the remainder of the proof we assume that $d = 2$.

The assumption (3.14) means that we can choose $\chi = \pi^h\,[F'_\varepsilon(\Psi^h)]$ in (3.28e) to yield, similarly to (3.21)–(3.23), with $\alpha = 0$ and F replaced by F_ε, on recalling (3.27), (3.9), (3.10), (3.30) and (3.28c,d), that

$$\begin{aligned}
&\frac{\mathrm{d}}{\mathrm{d}t}\,\left\langle F_\varepsilon(\Psi^h), 1\right\rangle^h_{\Gamma^h(t)} + \mathcal{D}_\Gamma\left\langle \nabla_s\,\Psi^h, \nabla_s\,\pi^h\,[F'_\varepsilon(\Psi^h)]\right\rangle_{\Gamma^h(t)}\\
&\qquad = \left\langle \nabla_s\,\vec{\mathrm{id}}, \nabla_s\,\pi^h\,[\gamma_\varepsilon(\Psi^h)\,\vec{\mathcal{V}}^h]\right\rangle_{\Gamma^h(t)} - \left\langle \nabla_s\,\pi^h\,[\gamma_\varepsilon(\Psi^h)], \vec{\mathcal{V}}^h\right\rangle_{\Gamma^h(t)}\\
&\qquad\quad + \left\langle \vec{\mathcal{V}}^h - \vec{\pi}^h\,\vec{U}^h, \nabla_s\,\pi^h\,[\gamma_\varepsilon(\Psi^h)]\right\rangle_{\Gamma^h(t)}\\
&\qquad = -\left\langle \kappa^h\,\vec{\nu}^h, \gamma_\varepsilon(\Psi^h)\,\vec{\mathcal{V}}^h\right\rangle^h_{\Gamma^h(t)} - \left\langle \vec{U}^h, \nabla_s\,\pi^h\,[\gamma_\varepsilon(\Psi^h)]\right\rangle^h_{\Gamma^h(t)}\\
&\qquad = -\left\langle \pi^h\,[\gamma_\varepsilon(\Psi^h)\,\kappa^h]\,\vec{\nu}^h, \vec{U}^h\right\rangle_{\Gamma^h(t)} - \left\langle \nabla_s\,\pi^h\,[\gamma_\varepsilon(\Psi^h)], \vec{U}^h\right\rangle^h_{\Gamma^h(t)}\,. \qquad (3.35)
\end{aligned}$$

Since $d = 2$ we can apply (3.16) to the function $G = F'_\varepsilon$, where we recall (3.14) and that $F_\varepsilon \in C^2(-\infty, \psi_\infty)$ is convex, and obtain that the second term on the left hand side of (3.35) is nonnegative. Hence the desired result (3.34) follows from combining (3.35) with (3.31). □

Clearly, (3.32), (3.33) and (3.34) are natural discrete analogues of (2.33), (2.32) and (2.31), respectively. We remark that the condition $\mathcal{X}_{\Omega^h_-(t)} \in \mathbb{P}^h(t)$ is always satisfied for the XFEM$_\Gamma$ approach as introduced in Barrett *et al.* (2013a,b).

In addition, it is possible to prove that the vertices of the solution $\Gamma^h(t)$ to (3.28a–e) are well distributed. As this follows already from the equations (3.28d), we refer to our earlier work in Barrett *et al.* (2007, 2008) for further details. In particular, we observe that in the case $d = 2$, i.e. for the planar two-phase problem, an equidistribution property for the vertices of $\Gamma^h(t)$ can be shown. These good mesh properties mean that for fully discrete schemes based on (3.28a–e) no remeshings are required in practice for either $d = 2$ or $d = 3$.

We remark that for the scheme (3.12a–e) it is not possible to prove (3.33), even if mass lumping was to be dropped from the right hand side of (3.12c), because $\vec{\chi} = \vec{\nu}^h$ is not a valid test function in (3.12c). As a consequence, the volume of the two phases will in general not be conserved in practice. This is an additional advantage of the formulation (3.28a–e) over (3.12a–e). A disadvantage is the fact that it does not appear possible to derive a discrete maximum principle similarly to (3.19). However, the following remark demonstrates that also for the scheme (3.28a–e) the negative part of Ψ^h can be controlled.

Moreover, in practice we observe that for a fully discrete variant of (3.28a–e) the fully discrete analogues of $\Psi^h(\cdot,t)$ remain positive for positive initial data.

REMARK. 3.6. *The convex nature of F, together with the fact that F' is singular at the origin, allows us to derive upper bounds on the negative part of Ψ^h for the two cases* (2.14a,b). *On recalling* (3.26a) *and* (2.12a), *it holds that*

$$F_\varepsilon(r) = \gamma(\varepsilon) + F'(\varepsilon)\, r + \tfrac{1}{2}\, F''(\varepsilon)\, (r-\varepsilon)^2 \geq \tfrac{1}{2}\, F''(\varepsilon)\, r^2 \geq \tfrac{1}{2}\, \varepsilon^{-1}\, \gamma_0\, \beta\, r^2 \qquad \forall\ r \leq 0\,,$$

provided that ε is sufficiently small. Hence the bound (3.34), *via a Korn's inequality, implies that*

$$\left\langle [\Psi^h]^2_-, 1 \right\rangle^h_{\Gamma^h(t)} \leq C\, \varepsilon \qquad \forall\ t \in (0,T] \qquad \textit{if} \quad \Psi^h(\cdot,0) \geq 0\,,$$

for some positive constant C, and for ε sufficiently small.

We recall that the stability proofs in Theorems 3.3 and 3.5 are restricted to the case $d = 2$. However, it is possible to prove stability for $d = 2$ and $d = 3$ for a variant of (3.12a–e), which, on recalling (2.23), is given by

$$\begin{aligned}
&\tfrac{1}{2}\left[\frac{\mathrm{d}}{\mathrm{d}t}\left(\rho^h\, \vec{U}^h, \vec{\xi}\right) + \left(\rho^h\, \vec{U}^h_t, \vec{\xi}\right) - \left(\rho^h\, \vec{U}^h, \vec{\xi}_t\right)\right] \\
&\quad + 2\left(\mu^h\, \underline{\underline{D}}(\vec{U}^h), \underline{\underline{D}}(\vec{\xi})\right) + \tfrac{1}{2}\left(\rho^h, [(\vec{I}^h_2\, \vec{U}^h \,.\, \nabla)\, \vec{U}^h] \,.\, \vec{\xi} - [(\vec{I}^h_2\, \vec{U}^h \,.\, \nabla)\, \vec{\xi}] \,.\, \vec{U}^h\right) \\
&\quad - \left(P^h, \nabla \,.\, \vec{\xi}\right) = \left(\rho^h\, \vec{f}^h_1 + \vec{f}^h_2, \vec{\xi}\right) - \left\langle \gamma(\Psi^h), \nabla_s \,.\, \vec{\pi}^h\, \vec{\xi} \right\rangle^h_{\Gamma^h(t)} \qquad \forall\ \vec{\xi} \in H^1(0,T;\mathbb{U}^h)\,,
\end{aligned} \tag{3.36}$$

together with (3.12b,c,e). Here we observe that in this new discretization it is no longer necessary to compute the discrete curvature vector $\vec{\kappa}^h$. It is then not difficult to prove the following theorem.

THEOREM. 3.7. *Let $\{(\Gamma^h, \vec{U}^h, P^h, \Psi^h)(t)\}_{t\in[0,T]}$ be a solution to* (3.36), (3.12b,c,e). *Then* (3.17) *and*

$$\tfrac{1}{2}\, \frac{\mathrm{d}}{\mathrm{d}t}\, \|[\rho^h]^{\frac{1}{2}}\, \vec{U}^h\|^2_0 + 2\, \|[\mu^h]^{\frac{1}{2}}\, \underline{\underline{D}}(\vec{U}^h)\|^2_0 = (\rho^h\, \vec{f}^h_1 + \vec{f}^h_2, \vec{U}^h) - \left\langle \gamma(\Psi^h), \nabla_s \,.\, \vec{\pi}^h\, \vec{U}^h \right\rangle^h_{\Gamma^h(t)} \tag{3.37}$$

hold. In addition, if $\mathcal{D}_\Gamma = 0$ or if (3.15) *and* (3.18) *hold, then we have* (3.19). *Moreover, if* (3.14) *and* (3.19) *hold, and $\mathcal{D}_\Gamma = 0$ or* (3.15) *holds, then*

$$\frac{\mathrm{d}}{\mathrm{d}t}\left(\tfrac{1}{2}\, \|[\rho^h]^{\frac{1}{2}}\, \vec{U}^h\|^2_0 + \left\langle F(\Psi^h), 1 \right\rangle^h_{\Gamma^h(t)}\right) + 2\, \|[\mu^h]^{\frac{1}{2}}\, \underline{\underline{D}}(\vec{U}^h)\|^2_0 \leq \left(\rho^h\, \vec{f}^h_1 + \vec{f}^h_2, \vec{U}^h\right). \tag{3.38}$$

Proof. The desired results (3.17) and (3.37) follow immediately on choosing $\chi = 1$ in (3.12e) and on choosing $\vec{\xi} = \vec{U}^h$ in (3.36) and $\varphi = P^h$ in (3.12b), respectively. The nonnegativity result (3.19) can be shown as in the proof of Theorem 3.3. The stability

bound (3.38) follows as in the proof of Theorem 3.3, on combining the first equation in (3.23) with (3.37) and $\vec{\mathcal{V}}^h = \vec{\pi}^h \vec{U}^h \,|_{\Gamma^h(t)}$, and on recalling that (3.24) holds if our assumptions are satisfied. We note that this proof is valid for $d = 3$, as we do not use (3.10). ∎

We recall that the assumption (3.15) always holds for $d = 2$, but for $d = 3$ it will in general only be satisfied if all the triangles $\sigma_j^h(t)$ of $\Gamma^h(t)$ have no obtuse angles. Unfortunately, in practice this will in general not be the case. Finally, we remark that it does not seem possible to derive a stability result for the scheme (3.36), (3.28b–e) in the case $d = 2$ or $d = 3$.

REMARK. 3.8. *We note that in the special case of constant surface tension, i.e. when* (2.15) *holds, then, similarly to* (2.30)*, the stability results* (3.20)*,* (3.34) *and* (3.38) *remain valid and reduce to*

$$\frac{\mathrm{d}}{\mathrm{d}t}\left(\tfrac{1}{2}\,\|[\rho^h]^{\frac{1}{2}}\,\vec{U}^h\|_0^2 + \gamma_0\,\mathcal{H}^{d-1}(\Gamma^h(t))\right) + 2\,\|[\mu^h]^{\frac{1}{2}}\,\underline{\underline{D}}(\vec{U}^h)\|_0^2 \leq \left(\rho^h\,\vec{f}_1^h + \vec{f}_2^h, \vec{U}^h\right), \quad (3.39)$$

where we note that $F_\varepsilon = F = \gamma_0$ *in* (3.34)*. The bound* (3.39) *recovers the stability results for the semidiscrete variants of the fully discrete schemes from Barrett* et al. *(2013b) for two-phase Navier–Stokes flow.*

3.2 Fully discrete approximation

In this section we consider fully discrete variants of the schemes (3.12a–e) and (3.28a–e) from §3.1. Here we will choose the time discretization such that existence and uniqueness of the discrete solutions can be guaranteed, and such that we inherit as much of the structure of the stable schemes in Barrett *et al.* (2013a,b) as possible, see below for details.

We consider the partitioning $t_m = m\,\tau$, $m = 0, \ldots, M$, of $[0, T]$ into uniform time steps $\tau = T/M$. The time discrete spatial discretizations then directly follow from the finite element spaces introduced in §3.1, where here in order to allow for local mesh refinements we consider bulk finite element spaces that change in time.

For all $m \geq 0$, let $\mathcal{T}^m$ be a regular partitioning of Ω into disjoint open simplices o_j^m, $j = 1, \ldots, J_\Omega^m$. We set $h^m := \max_{j=1,\ldots,J_\Omega^m} \mathrm{diam}(o_j^m)$. Associated with $\mathcal{T}^m$ are the finite element spaces S_k^m for $k \geq 0$. We introduce also $\vec{I}_k^m : [C(\overline{\Omega})]^d \to [S_k^m]^d$, $k \geq 1$, the standard interpolation operators, and the standard projection operator $I_0^m : L^1(\Omega) \to S_0^m$. For the approximation to the velocity and pressure on $\mathcal{T}^m$ will use the finite element spaces $\mathbb{U}^m \subset \mathbb{U}$ and $\mathbb{P}^m \subset \mathbb{P}$, which are the direct time discrete analogues of $\mathbb{U}^h$ and $\mathbb{P}^h(t_m)$, as well as $\widehat{\mathbb{P}}^m \subset \widehat{\mathbb{P}}$. We recall that $(\mathbb{U}^m, \mathbb{P}^m)$ are said to satisfy the LBB inf-sup condition if there exists a constant $C_0 \in \mathbb{R}_{>0}$ independent of h^m such that

$$\inf_{\varphi \in \widehat{\mathbb{P}}^m} \sup_{\vec{\xi} \in \mathbb{U}^m} \frac{(\varphi, \nabla \,.\, \vec{\xi})}{\|\varphi\|_0\,\|\vec{\xi}\|_1} \geq C_0\,. \quad (3.40)$$

Similarly, the parametric finite element spaces are given by

$$\underline{V}(\Gamma^m) := \{\vec{\chi} \in [C(\Gamma^m)]^d : \vec{\chi}|_{\sigma_j^m} \text{ is linear } \forall\ j = 1, \ldots, J_\Gamma\} =: [W(\Gamma^m)]^d\,,$$

for $m = 0, \ldots, M-1$. Here $\Gamma^m = \bigcup_{j=1}^{J_\Gamma} \overline{\sigma_j^m}$, where $\{\sigma_j^m\}_{j=1}^{J_\Gamma}$ is a family of mutually disjoint open $(d-1)$-simplices with vertices $\{\vec{q}_k^m\}_{k=1}^{K_\Gamma}$. We denote the standard basis of $W(\Gamma^m)$ by $\{\chi_k^m(\cdot,t)\}_{k=1}^{K_\Gamma}$. We also introduce $\pi^m : C(\Gamma^m) \to W(\Gamma^m)$, the standard interpolation operator at the nodes $\{\vec{q}_k^m\}_{k=1}^{K_\Gamma}$, and similarly $\vec{\pi}^m : [C(\Gamma^m)]^d \to \underline{V}(\Gamma^m)$. Throughout this paper, we will parameterize the new closed surface Γ^{m+1} over Γ^m, with the help of a parameterization $\vec{X}^{m+1} \in \underline{V}(\Gamma^m)$, i.e. $\Gamma^{m+1} = \vec{X}^{m+1}(\Gamma^m)$. Moreover, for $m \geq 0$, we will use the notation $\vec{X}^m = \vec{\mathrm{id}}\,|_{\Gamma^m} \in \underline{V}(\Gamma^m)$.

We also introduce the L^2–inner product $\langle\cdot,\cdot\rangle_{\Gamma^m}$ over the current polyhedral surface Γ^m, as well as the the mass lumped inner product $\langle\cdot,\cdot\rangle_{\Gamma^m}^h$. Given Γ^m, we let Ω_+^m denote the exterior of Γ^m and let Ω_-^m denote the interior of Γ^m, so that $\Gamma^m = \partial\Omega_-^m = \overline{\Omega_-^m} \cap \overline{\Omega_+^m}$. We then partition the elements of the bulk mesh $\mathcal{T}^m$ into interior, exterior and interfacial elements as before, and we introduce ρ^m, $\mu^m \in S_0^m$, for $m \geq 0$, as

$$\rho^m|_{o^m} = \begin{cases} \rho_- & o^m \in \mathcal{T}_-^m\,, \\ \rho_+ & o^m \in \mathcal{T}_+^m\,, \\ \frac{1}{2}(\rho_- + \rho_+) & o^m \in \mathcal{T}_{\Gamma^m}^m\,, \end{cases} \quad \text{and} \quad \mu^m|_{o^m} = \begin{cases} \mu_- & o^m \in \mathcal{T}_-^m\,, \\ \mu_+ & o^m \in \mathcal{T}_+^m\,, \\ \frac{1}{2}(\mu_- + \mu_+) & o^m \in \mathcal{T}_{\Gamma^m}^m\,. \end{cases} \tag{3.41}$$

We also set $\rho^{-1} := \rho^0$.

Our proposed fully discrete equivalent of (3.12a–e) is then given as follows. Let Γ^0, an approximation to $\Gamma(0)$, and $\vec{U}^0 \in \mathbb{U}^0$, as well as $\vec{\kappa}^0 \in \underline{V}(\Gamma^0)$ and $\Psi^0 \in W(\Gamma^0)$ be given. For $m = 0, \ldots, M-1$, find $\vec{U}^{m+1} \in \mathbb{U}^m$, $P^{m+1} \in \widehat{\mathbb{P}}^m$, $\vec{X}^{m+1} \in \underline{V}(\Gamma^m)$ and $\vec{\kappa}^{m+1} \in \underline{V}(\Gamma^m)$ such that

$$\begin{aligned} &\tfrac{1}{2}\left(\frac{\rho^m\,\vec{U}^{m+1} - (I_0^m\,\rho^{m-1})\,\vec{I}_2^m\,\vec{U}^m}{\tau} + (I_0^m\,\rho^{m-1})\,\frac{\vec{U}^{m+1} - \vec{I}_2^m\,\vec{U}^m}{\tau}, \vec{\xi}\right) \\ &\qquad + 2\left(\mu^m\,\underline{\underline{D}}(\vec{U}^{m+1}), \underline{\underline{D}}(\vec{\xi})\right) + \tfrac{1}{2}\left(\rho^m, [(\vec{I}_2^m\,\vec{U}^m\,.\,\nabla)\,\vec{U}^{m+1}]\,.\,\vec{\xi} - [(\vec{I}_2^m\,\vec{U}^m\,.\,\nabla)\,\vec{\xi}]\,.\,\vec{U}^{m+1}\right) \\ &\qquad - \left(P^{m+1}, \nabla\,.\,\vec{\xi}\right) = \left(\rho^m\,\vec{f}_1^{m+1} + \vec{f}_2^{m+1}, \vec{\xi}\right) + \left\langle \gamma(\Psi^m)\,\vec{\kappa}^m + \nabla_s\,\pi^m\,[\gamma(\Psi^m)], \vec{\xi}\right\rangle_{\Gamma^m}^h \\ &\qquad\qquad \forall\ \vec{\xi} \in \mathbb{U}^m\,, \end{aligned} \tag{3.42a}$$

$$\left(\nabla\,.\,\vec{U}^{m+1}, \varphi\right) = 0 \qquad \forall\ \varphi \in \widehat{\mathbb{P}}^m\,, \tag{3.42b}$$

$$\left\langle \frac{\vec{X}^{m+1} - \vec{X}^m}{\tau}, \vec{\chi}\right\rangle_{\Gamma^m}^h = \left\langle \vec{U}^{m+1}, \vec{\chi}\right\rangle_{\Gamma^m}^h \qquad \forall\ \vec{\chi} \in \underline{V}(\Gamma^m)\,, \tag{3.42c}$$

$$\left\langle \vec{\kappa}^{m+1}, \vec{\eta}\right\rangle_{\Gamma^m}^h + \left\langle \nabla_s\,\vec{X}^{m+1}, \nabla_s\,\vec{\eta}\right\rangle_{\Gamma^m} = 0 \qquad \forall\ \vec{\eta} \in \underline{V}(\Gamma^m) \tag{3.42d}$$

and set $\Gamma^{m+1} = \vec{X}^{m+1}(\Gamma^m)$. We note that in (3.42a), as no confusion can arise, for $m \geq 1$ we denote by $\vec{\kappa}^m$ the function $\vec{z} \in \underline{V}(\Gamma^m)$, defined by $\vec{z}(\vec{q}_k^{\,m}) = \vec{\kappa}^m(\vec{q}_k^{\,m-1})$, $k = 1, \ldots, K_\Gamma$, where $\vec{\kappa}^m \in \underline{V}(\Gamma^{m-1})$ is given. Then find $\Psi^{m+1} \in W(\Gamma^{m+1})$ such that

$$\frac{1}{\tau} \left\langle \Psi^{m+1}, \chi_k^{m+1} \right\rangle_{\Gamma^{m+1}}^h + \mathcal{D}_\Gamma \left\langle \nabla_s \Psi^{m+1}, \nabla_s \chi_k^{m+1} \right\rangle_{\Gamma^{m+1}} = \frac{1}{\tau} \left\langle \Psi^m, \chi_k^m \right\rangle_{\Gamma^m}^h \quad \forall\ k \in \{1, \ldots, K_\Gamma\}\,. \tag{3.42e}$$

Here we have defined $\vec{f}_i^{\,m+1} := \vec{I}_2^{\,m} \vec{f}_i(\cdot, t_{m+1})$, $i = 1, 2$. We observe that (3.42a–e) is a linear scheme in that it leads to a linear system of equations for the unknowns $(\vec{U}^{m+1}, P^{m+1}, \vec{X}^{m+1}, \vec{\kappa}^{m+1}, \Psi^{m+1})$ at each time level. In particular, the system (3.42a–e) clearly decouples into (3.42a,b) for $(\vec{U}^{m+1}, P^{m+1})$, then (3.42c,d) for $(\vec{X}^{m+1}, \vec{\kappa}^{m+1})$ and finally (3.42e) for Ψ^{m+1}.

REMARK. 3.9. *Of course, the natural analogue of* (3.42a–e) *that is based on the semidiscrete scheme from* Theorem 3.7*, is given by: Find* $\vec{U}^{m+1} \in \mathbb{U}^m$*,* $P^{m+1} \in \widehat{\mathbb{P}}^m$*,* $\vec{X}^{m+1} \in \underline{V}(\Gamma^m)$ *and* $\Psi^{m+1} \in W(\Gamma^{m+1})$ *such that* (3.42a–c,e) *hold with* $\langle \gamma(\Psi^m)\, \vec{\kappa}^m + \nabla_s\, \pi^m\, [\gamma(\Psi^m)], \vec{\xi} \rangle_{\Gamma^m}^h$ *in* (3.42a) *replaced by* $-\langle \gamma(\Psi^m), \nabla_s \,.\, \vec{\pi}^m\, \vec{\xi} \rangle_{\Gamma^m}^h$.

When the velocity/pressure space pair $(\mathbb{U}^m, \widehat{\mathbb{P}}^m)$ does not satisfy (3.40), we need to consider the following reduced version of (3.42a,b), where the pressure P^{m+1} is eliminated, in order to prove existence of a solution. Let

$$\mathbb{U}_0^m := \{\vec{U} \in \mathbb{U}^m : (\nabla \,.\, \vec{U}, \varphi) = 0 \ \ \forall\ \varphi \in \widehat{\mathbb{P}}^m\}\,.$$

Then any solution $(\vec{U}^{m+1}, P^{m+1}) \in \mathbb{U}^m \times \widehat{\mathbb{P}}^m$ to (3.42a,b) is such that $\vec{U}^{m+1} \in \mathbb{U}_0^m$ satisfies (3.42a) with $\mathbb{U}^m$ replaced by $\mathbb{U}_0^m$. In addition, we make the following very mild well-posedness assumption.

($\mathcal{A}$) We assume for $m = 0, \ldots, M-1$ that $\mathcal{H}^{d-1}(\sigma_j^m) > 0$ for all $j = 1, \ldots, J_\Gamma$, and that $\Gamma^m \subset \Omega$.

Moreover, and similarly to (3.15), we note that the assumption

$$\int_{\sigma_j^{m+1}} \nabla_s \chi_i^{m+1} \,.\, \nabla_s \chi_k^{m+1}\, \mathrm{d}\mathcal{H}^{d-1} \leq 0 \quad \forall\ i \neq k\,, \qquad j = 1, \ldots, J_\Gamma \tag{3.43}$$

is always satisfied for $d = 2$, and for $d = 3$ if all the triangles σ^{m+1} of Γ^{m+1} have no obtuse angles.

THEOREM. 3.10. *Let the assumption* ($\mathcal{A}$) *hold. If the LBB condition* (3.40) *holds, then there exists a unique solution* $(\vec{U}^{m+1}, P^{m+1}) \in \mathbb{U}^m \times \widehat{\mathbb{P}}^m$ *to* (3.42a,b)*. In all other cases there exists a unique solution* $\vec{U}^{m+1} \in \mathbb{U}_0^m$ *to the reduced equation* (3.42a) *with* $\mathbb{U}^m$ *replaced by* $\mathbb{U}_0^m$*. In either case, there exists a unique solution* $(\vec{X}^{m+1}, \vec{\kappa}^{m+1}) \in \underline{V}(\Gamma^m) \times \underline{V}(\Gamma^m)$ *to* (3.42c,d)*. Finally, there exists a unique solution* $\Psi^{m+1} \in W(\Gamma^{m+1})$ *to* (3.42e) *that satisfies*

$$\left\langle \Psi^{m+1}, 1 \right\rangle_{\Gamma^{m+1}} = \left\langle \Psi^m, 1 \right\rangle_{\Gamma^m} \tag{3.44a}$$

and, if $\mathcal{D}_\Gamma = 0$ *or if the assumption* (3.43) *holds,*

$$\Psi^{m+1} \geq 0 \qquad \textit{if} \quad \Psi^m \geq 0\,. \tag{3.44b}$$

Proof. As all the systems are linear, existence follows from uniqueness. In order to establish the latter, we will consider the homogeneous system in each case. We begin with: Find $(\vec{U}, P) \in \mathbb{U}^m \times \widehat{\mathbb{P}}^m$ such that

$$\begin{aligned}
&\tfrac{1}{2\tau}\left((\rho^m + I_0^m\,\rho^{m-1})\,\vec{U}, \vec{\xi}\right) + 2\left(\mu^m\,\underline{\underline{D}}(\vec{U}), \underline{\underline{D}}(\vec{\xi})\right) - \left(P, \nabla\,.\,\vec{\xi}\right) \\
&\qquad + \tfrac{1}{2}\left(\rho^m, [(\vec{I}_2^m\,\vec{U}^m\,.\,\nabla)\,\vec{U}]\,.\,\vec{\xi} - [(\vec{I}_2^m\,\vec{U}^m\,.\,\nabla)\,\vec{\xi}]\,.\,\vec{U}\right) = 0 \qquad \forall\ \vec{\xi} \in \mathbb{U}^m\,, \qquad \text{(3.45a)} \\
&\left(\nabla\,.\,\vec{U}, \varphi\right) = 0 \qquad \forall\ \varphi \in \widehat{\mathbb{P}}^m\,. \qquad \text{(3.45b)}
\end{aligned}$$

Choosing $\vec{\xi} = \vec{U}$ in (3.45a) and $\varphi = P$ in (3.45b) yields that

$$\tfrac{1}{2}\left((\rho^m + I_0^m\,\rho^{m-1})\,\vec{U}, \vec{U}\right) + 2\,\tau\left(\mu^m\,\underline{\underline{D}}(\vec{U}), \underline{\underline{D}}(\vec{U})\right) = 0\,. \tag{3.46}$$

It immediately follows from (3.46), on recalling $\rho_\pm > 0$, that $\vec{U} = \vec{0} \in \mathbb{U}^m$. Moreover, (3.45a) with $\vec{U} = \vec{0}$ implies, together with (3.40), that $P = 0 \in \widehat{\mathbb{P}}^m$. This shows existence and uniqueness of $(\vec{U}^{m+1}, P^{m+1}) \in \mathbb{U}^m \times \widehat{\mathbb{P}}^m$. The proof for the reduced equation is very similar. The homogeneous system to consider is (3.45a) with $\mathbb{U}^m$ replaced by $\mathbb{U}_0^m$, where we note that the latter is a linear subspace of $\mathbb{U}^m$. As before, (3.46) yields that $\vec{U} = \vec{0} \in \mathbb{U}_0^m$, and so the existence of a unique solution $\vec{U}^{m+1} \in \mathbb{U}_0^m$ to the reduced equation.

Next we consider: Find $(\vec{X}, \vec{\kappa}) \in \underline{V}(\Gamma^m) \times \underline{V}(\Gamma^m)$ such that

$$\begin{aligned}
&\left\langle \vec{X}, \vec{\chi} \right\rangle_{\Gamma^m}^h = 0 \qquad \forall\ \vec{\chi} \in \underline{V}(\Gamma^m)\,, \\
&\langle \vec{\kappa}, \vec{\eta} \rangle_{\Gamma^m}^h + \left\langle \nabla_s\,\vec{X}, \nabla_s\,\vec{\eta} \right\rangle_{\Gamma^m} = 0 \qquad \forall\ \vec{\eta} \in \underline{V}(\Gamma^m)\,,
\end{aligned}$$

which immediately implies that $\vec{X} = \vec{0}$ and hence $\vec{\kappa} = \vec{0}$. Finally, (3.42e) is clearly a symmetric, positive definite linear system with a unique solution $\Psi^{m+1} \in W(\Gamma^{m+1})$. The desired result (3.44a) follows on summing (3.42e) for $k = 1, \ldots, K_\Gamma$. In order to prove (3.44b) we assume that $\Psi^m \geq 0$ and observe from (3.42e) that this implies that

$$\left\langle \Psi^{m+1}, [\Psi^{m+1}]_- \right\rangle_{\Gamma^{m+1}}^h + \tau\,\mathcal{D}_\Gamma\left\langle \nabla_s\,\Psi^{m+1}, \nabla_s\,\pi^{m+1}\,[\Psi^{m+1}]_- \right\rangle_{\Gamma^{m+1}} \leq 0\,. \tag{3.47}$$

Similarly to (3.16) it follows that under our assumptions the second term in (3.47) is nonnegative, which yields that

$$\left\langle [\Psi^{m+1}]_-, [\Psi^{m+1}]_- \right\rangle_{\Gamma^{m+1}}^h = \left\langle \Psi^{m+1}, [\Psi^{m+1}]_- \right\rangle_{\Gamma^{m+1}}^h \leq 0\,,$$

i.e. $\Psi^{m+1} \geq 0$. ∎

Our proposed fully discrete equivalent of (3.28a–e) is given as follows, where we recall the regularization parameter $\varepsilon > 0$ and the definitions (3.26a,b). Let Γ^0, an approximation to $\Gamma(0)$, and $\vec{U}^0 \in \mathbb{U}^0$, as well as $\kappa^0 \in W(\Gamma^0)$ and $\Psi^0 \in W(\Gamma^0)$ be given. For $m = 0, \ldots, M-1$, find $\vec{U}^{m+1} \in \mathbb{U}^m$, $P^{m+1} \in \widehat{\mathbb{P}}^m$, $\vec{X}^{m+1} \in \underline{V}(\Gamma^m)$ and $\kappa^{m+1} \in W(\Gamma^m)$ such that

$$\begin{aligned}
&\tfrac{1}{2}\left(\frac{\rho^m\,\vec{U}^{m+1} - (I_0^m\,\rho^{m-1})\,\vec{I}_2^m\,\vec{U}^m}{\tau} + (I_0^m\,\rho^{m-1})\,\frac{\vec{U}^{m+1} - \vec{I}_2^m\,\vec{U}^m}{\tau}, \vec{\xi}\right) \\
&\qquad + 2\left(\mu^m\,\underline{\underline{D}}(\vec{U}^{m+1}), \underline{\underline{D}}(\vec{\xi})\right) + \tfrac{1}{2}\left(\rho^m, [(\vec{I}_2^m\,\vec{U}^m\,.\,\nabla)\,\vec{U}^{m+1}]\,.\,\vec{\xi} - [(\vec{I}_2^m\,\vec{U}^m\,.\,\nabla)\,\vec{\xi}]\,.\,\vec{U}^{m+1}\right) \\
&\qquad - \left(P^{m+1}, \nabla\,.\,\vec{\xi}\right) = \left(\rho^m\,\vec{f}_1^{m+1} + \vec{f}_2^{m+1}, \vec{\xi}\right) + \left\langle \pi^m\,[\gamma_\varepsilon(\Psi^m)\,\kappa^m]\,\vec{\nu}^m, \vec{\xi}\right\rangle_{\Gamma^m} \\
&\qquad\qquad + \left\langle \nabla_s\,\pi^m\,[\gamma_\varepsilon(\Psi^m)], \vec{\xi}\right\rangle^h_{\Gamma^m} \qquad \forall\ \vec{\xi} \in \mathbb{U}^m\,, \qquad (3.48a)
\end{aligned}$$

$$\left(\nabla\,.\,\vec{U}^{m+1}, \varphi\right) = 0 \quad \forall\ \varphi \in \widehat{\mathbb{P}}^m\,, \qquad (3.48b)$$

$$\left\langle \frac{\vec{X}^{m+1} - \vec{X}^m}{\tau}, \chi\,\vec{\nu}^m \right\rangle^h_{\Gamma^m} = \left\langle \vec{U}^{m+1}, \chi\,\vec{\nu}^m \right\rangle_{\Gamma^m} \quad \forall\ \chi \in W(\Gamma^m)\,, \qquad (3.48c)$$

$$\left\langle \kappa^{m+1}\,\vec{\nu}^m, \vec{\eta}\right\rangle^h_{\Gamma^m} + \left\langle \nabla_s\,\vec{X}^{m+1}, \nabla_s\,\vec{\eta}\right\rangle_{\Gamma^m} = 0 \quad \forall\ \vec{\eta} \in \underline{V}(\Gamma^m) \qquad (3.48d)$$

and set $\Gamma^{m+1} = \vec{X}^{m+1}(\Gamma^m)$. We note that in (3.48a), similarly to $\vec{\kappa}^m$ in (3.42a), for $m \geq 1$ we denote by κ^m the function $z \in W(\Gamma^m)$, defined by $z(\vec{q}_k^m) = \kappa^m(\vec{q}_k^{m-1})$, $k = 1, \ldots, K_\Gamma$, where $\kappa^m \in W(\Gamma^{m-1})$ is given. Then find $\Psi^{m+1} \in W(\Gamma^{m+1})$ such that

$$\begin{aligned}
&\frac{1}{\tau}\left\langle \Psi^{m+1}, \chi_k^{m+1}\right\rangle^h_{\Gamma^{m+1}} + \mathcal{D}_\Gamma\left\langle \nabla_s\,\Psi^{m+1}, \nabla_s\,\chi_k^{m+1}\right\rangle_{\Gamma^{m+1}} \\
&\quad = \frac{1}{\tau}\left\langle \Psi^m, \chi_k^m\right\rangle^h_{\Gamma^m} - \left\langle \Psi^m_{\star,\varepsilon}\left(\frac{\vec{X}^{m+1} - \vec{X}^m}{\tau} - \vec{U}^{m+1}\right), \nabla_s\,\chi_k^m\right\rangle^h_{\Gamma^m} \qquad \forall\ k \in \{1, \ldots, K_\Gamma\}\,,
\end{aligned} \qquad (3.48e)$$

where $\Psi^m_{\star,\varepsilon} = \Psi^m$ for $d = 3$ and, similarly to (3.29),

$$\Psi^m_{\star,\varepsilon} = \begin{cases} -\frac{\gamma_\varepsilon(\Psi^m_k) - \gamma_\varepsilon(\Psi^m_{k-1})}{F'_\varepsilon(\Psi^m_k) - F'_\varepsilon(\Psi^m_{k-1})} & F'_\varepsilon(\Psi^m_{k-1}) \neq F'_\varepsilon(\Psi^m_k)\,, \\ \frac{1}{2}\,(\Psi^m_{k-1} + \Psi^m_k) & F'_\varepsilon(\Psi^m_{k-1}) = F'_\varepsilon(\Psi^m_k)\,, \end{cases} \quad \text{on} \quad [\vec{q}^m_{k-1}, \vec{q}^m_k] \quad \forall\ k \in \{1, \ldots, K_\Gamma\}$$

for $d = 2$, where $\Psi^m = \sum_{k=1}^{K_\Gamma} \Psi^m_k\,\chi^m_k$. We observe that (3.48a–e) is a linear scheme in that it leads to a linear system of equations for the unknowns $(\vec{U}^{m+1}, P^{m+1}, \vec{X}^{m+1}, \kappa^{m+1}, \Psi^{m+1})$ at each time level. In particular, the system (3.48a–e) clearly decouples into (3.48a,b) for $(\vec{U}^{m+1}, P^{m+1})$, then (3.48c,d) for $(\vec{X}^{m+1}, \kappa^{m+1})$ and finally (3.48e) for Ψ^{m+1}.

In order to prove the existence of a unique solution to (3.48c,d) we need to make the following very mild additional assumption.

($\mathcal{B}$) For $k = 1, \dots, K_\Gamma$, let $\Xi_k^m := \{\sigma_j^m : \vec{q}_k^m \in \overline{\sigma_j^m}\}$ and set

$$\Lambda_k^m := \bigcup_{\sigma_j^m \in \Xi_k^m} \overline{\sigma_j^m} \qquad \text{and} \qquad \vec{\omega}_k^m := \frac{1}{\mathcal{H}^{d-1}(\Lambda_k^m)} \sum_{\sigma_j^m \in \Xi_k^m} \mathcal{H}^{d-1}(\sigma_j^m)\, \vec{\nu}_j^m \,.$$

Then we further assume that $\dim \operatorname{span}\{\vec{\omega}_k^m\}_{k=1}^{K_\Gamma} = d$, $m = 0, \dots, M-1$.

We refer to Barrett *et al.* (2007) and Barrett *et al.* (2008) for more details and for an interpretation of this assumption, but we note that ($\mathcal{B}$) is always satisfied if Γ^m has no self-intersections. Given the above definitions, we introduce the piecewise linear vertex normal function

$$\vec{\omega}^m := \sum_{k=1}^{K_\Gamma} \chi_k^m\, \vec{\omega}_k^m \in \underline{V}(\Gamma^m)\,,$$

and note that

$$\langle \vec{v}, w\, \vec{\nu}^m \rangle_{\Gamma^m}^h = \langle \vec{v}, w\, \vec{\omega}^m \rangle_{\Gamma^m}^h \qquad \forall\ \vec{v} \in \underline{V}(\Gamma^m)\,,\ w \in W(\Gamma^m)\,. \tag{3.49}$$

THEOREM. 3.11. *Let the assumption* ($\mathcal{A}$) *hold. If the LBB condition* (3.40) *holds, then there exists a unique solution* $(\vec{U}^{m+1}, P^{m+1}) \in \mathbb{U}^m \times \widehat{\mathbb{P}}^m$ *to* (3.48a,b). *In all other cases there exists a unique solution* $\vec{U}^{m+1} \in \mathbb{U}_0^m$ *to the reduced equation* (3.48a) *with* $\mathbb{U}^m$ *replaced by* $\mathbb{U}_0^m$. *If the assumption* ($\mathcal{B}$) *holds, then there exists a unique solution* $(\vec{X}^{m+1}, \kappa^{m+1}) \in \underline{V}(\Gamma^m) \times W(\Gamma^m)$ *to* (3.48c,d). *Finally, there exists a unique solution* $\Psi^{m+1} \in W(\Gamma^{m+1})$ *to* (3.48e) *that satisfies* (3.44a).

Proof. The results for $\vec{U}^{m+1}$, P^{m+1} and Ψ^{m+1} can be shown exactly as in the proof of Theorem 3.10. For the remaining result we consider: Find $(\vec{X}, \kappa) \in \underline{V}(\Gamma^m) \times W(\Gamma^m)$ such that

$$\left\langle \vec{X}, \chi\, \vec{\nu}^m \right\rangle_{\Gamma^m}^h = 0 \qquad \forall\ \chi \in W(\Gamma^m)\,, \tag{3.50a}$$

$$\langle \kappa\, \vec{\nu}^m, \vec{\eta} \rangle_{\Gamma^m}^h + \left\langle \nabla_s\, \vec{X}, \nabla_s\, \vec{\eta} \right\rangle_{\Gamma^m} = 0 \qquad \forall\ \vec{\eta} \in \underline{V}(\Gamma^m)\,. \tag{3.50b}$$

Choosing $\chi = \kappa$ in (3.50a) and $\vec{\eta} = \vec{X}$ in (3.50b) yields that

$$\left\langle \nabla_s\, \vec{X}, \nabla_s\, \vec{X} \right\rangle_{\Gamma^m} = 0\,. \tag{3.51}$$

It immediately follows from (3.51) that $\vec{X} = \vec{X}_c \in \mathbb{R}^d$. Together with (3.50a), (3.49) and the assumption ($\mathcal{B}$) this yields that $\vec{X} = \vec{0}$. Now (3.50b) with $\vec{\eta} = \vec{\pi}^m[\kappa\, \vec{\omega}^m]$, recall (3.49), implies that $\kappa = 0$. □

REMARK. 3.12. *On replacing* κ^m *in* (3.48a) *with* κ^{m+1} *the subsystem* (3.48a–d) *no longer decouples. However, this system, for the special case of constant surface tension, as in* (2.15), *i.e. for a two-phase flow problem without surfactants, has been considered by the authors in Barrett* et al. *(2013b). For this finite element approximation of two-phase*

flow, the authors proved the existence of a unique solution $(\vec{U}^{m+1}, \vec{X}^{m+1}, \kappa^{m+1}) \in \mathbb{U}_0^m \times \underline{V}(\Gamma^m) \times W(\Gamma^m)$ *to the reduced system* (3.48a,c,d)*, with* $\mathbb{U}^m$ *replaced by* $\mathbb{U}_0^m$*, and with* κ^m *in* (3.48a) *replaced by* κ^{m+1}*, which in addition satisfies the following stability bound:*

$$\begin{aligned}\tfrac{1}{2}\,(\rho^m\,\vec{U}^{m+1},\vec{U}^{m+1}) + \gamma_0\,\mathcal{H}^{d-1}(\Gamma^{m+1}) + \tfrac{1}{2}\left((I_0^m\rho^{m-1})\,(\vec{U}^{m+1}-\vec{I}_2^m\,\vec{U}^m),\vec{U}^{m+1}-\vec{I}_2^m\,\vec{U}^m\right)\\ + 2\,\tau\left(\mu^m\,\underline{\underline{D}}(U^{m+1}),\underline{\underline{D}}(U^{m+1})\right)\\ \leq \tfrac{1}{2}\,(I_0^m\,\rho^{m-1}\,\vec{I}_2^m\,\vec{U}^m,\vec{I}_2^m\,\vec{U}^m) + \gamma_0\,\mathcal{H}^{d-1}(\Gamma^m) + \tau\left(\rho^m\,\vec{f}_1^{m+1}+\vec{f}_2^{m+1},\vec{U}^{m+1}\right).\end{aligned}$$

The same stability result, in the case (2.15)*, can be shown for the scheme* (3.42a–e)*, once again on replacing* $\vec{\kappa}^m$ *in* (3.42a) *with* $\vec{\kappa}^{m+1}$*.*

The above remark motivates our choice of time discretizations in (3.48a–d). As it does not appear possible to prove a stability result similar to (3.34) for the fully discrete scheme (3.48a–e) for general choices of γ such as (2.14a,b), we prefer to use κ^m in (3.48a) rather than κ^{m+1}, which simplifies the existence and uniqueness proof, as well as the solution procedure.

Remark. 3.13. *For ease of presentation we have assumed so far that the number of vertices,* K_Γ*, and the number of elements,* J_Γ*, of the discrete interface* Γ^m *remain constant over time. However, it is a simple matter to allow for a localized refinement procedure as employed in Barrett* et al. *(2013b). Here any newly introduced basis function for* Γ^{m+1}*, say, needs to be traced back to* Γ^m *so that* (3.48e)*, and similarly* (3.42e)*, remain well-defined.*

4 Numerical results

For details on the assembly of the linear system arising at each time step of (3.48a–e), as well as details on the adaptive mesh refinement algorithm and the solution procedure, we refer to Barrett *et al.* (2013b). The main new ingredient is (3.48e), which decouples from (3.48a–d) and so is straightforward to solve. An analogous comment holds for the scheme (3.42a–e). We recall from Barrett *et al.* (2013b) that for the bulk mesh adaptation we use a strategy that results in a fine mesh size h_f around Γ^m and a coarse mesh size h_c further away from it. Here $h_f = \frac{2\,\min\{H_1,H_2\}}{N_f}$ and $h_c = \frac{2\,\min\{H_1,H_2\}}{N_c}$ are given by two integer numbers $N_f > N_c$, where we assume from now on that Ω is given by $\times_{i=1}^d(-H_i,H_i)$. We remark that we implemented our scheme with the help of the finite element toolbox ALBERTA, see Schmidt and Siebert (2005).

For the scheme (3.48a–e) we fix $\varepsilon = 10^{-5}$, and in all our numerical experiments presented in this section the discrete surfactant concentration Ψ^m remained above ε throughout the evolution, so that $\gamma_\varepsilon(\Psi^m) = \gamma(\Psi^m)$, recall (3.26b). Unless otherwise stated we use the linear equation of state (2.14a) for the surface tension, and for the numerical simulations without surfactant we set $\beta = 0$ in (2.14a). We set $\Psi^0 = \psi_0 = 1$, unless

stated otherwise. In addition, we employ the lowest order Taylor–Hood element P2–P1 in all computations and set $\vec{U}^0 = \vec{I}_2^h \, \vec{u}_0$, where $\vec{u}_0 = \vec{0}$ unless stated otherwise. For the initial interface we always choose a circle/sphere of radius R_0 and set $\kappa^0 = -\frac{d-1}{R_0}$ for the scheme (3.48a–e). For the scheme (3.42a–e) we let $\vec{\kappa}^0 \in \underline{V}(\Gamma^0)$ be the solution of (3.42d) with m and $m+1$ replaced by zero. To summarize the discretization parameters we use the shorthand notation $n\,\text{adapt}_{k,l}$ from Barrett *et al.* (2013b). The subscripts refer to the fineness of the spatial discretizations, i.e. for the set $n\,\text{adapt}_{k,l}$ it holds that $N_f = 2^k$ and $N_c = 2^l$. For the case $d = 2$ we have in addition that $K_\Gamma = J_\Gamma = 2^k$, while for $d = 3$ it holds that $(K_\Gamma, J_\Gamma) = (770, 1536), (1538, 3072), (3074, 6144)$ for $k = 5, 6, 7$. Finally, the uniform time step size for the set $n\,\text{adapt}_{k,l}$ is given by $\tau = 10^{-3}/n$, and if $n = 1$ we write $\text{adapt}_{k,l}$.

4.1 Convergence experiments for convection diffusion equation

In this subsection we test the two approximations (3.42c,e) and (3.48c–e) for the convection diffusion equation (2.9), in a situation where the evolution of the surface $\Gamma(t)$ is given. In particular, we perform convergence experiments for the true solution from the Appendix; that is, $\psi(\vec{z}, t) = e^{-6\,t}\, z_1\, z_2$ is fixed on the moving ellipsoid $\Gamma(t)$ with time dependent x_1-axis. To this end, we replace $\vec{U}^{m+1}$ in (3.42c) and (3.48c,e) with $\vec{u}(\cdot, t_{m+1})$ as defined in (A.2), and set $\mathcal{D}_\Gamma = 1$. In addition, we add the term

$$\left\langle f_\Gamma^{m+1}, \chi_k^{m+1} \right\rangle_{\Gamma^{m+1}}^h$$

to the right hand sides of (3.42e) and (3.48e), where $f_\Gamma^{m+1} \in W(\Gamma^{m+1})$ is defined such that

$$f_\Gamma^{m+1}(\vec{q}_k^{m+1}) = f_\Gamma(\vec{\Pi}_{\Gamma(t_{m+1})}\, \vec{q}_k^{m+1}, t_{m+1}) \qquad k = 1, \ldots, K_\Gamma\,,$$

with f_Γ given as in (A.3), and with $\vec{\Pi}_{\Gamma(t)} : \mathbb{R}^d \to \Gamma(t)$ denoting the orthogonal projection onto $\Gamma(t)$ for $t \in [0, T]$. In practice this projection can be computed with the help of a Newton iteration. In Tables 1 and 2 we report on the error

$$\|\Psi - \psi\|_{L^2} := \left[\sum_{m=1}^{M} \tau \left\langle [\Psi^m - \psi(\cdot, t_m) \circ \vec{\Pi}_{\Gamma(t_m)}]^2, 1 \right\rangle_{\Gamma^m}^h \right]^{\frac{1}{2}}$$

for convergence experiments for $d = 2$ and $d = 3$, respectively. Here we choose the time interval $[0, T]$ with $T = 1$, and for the uniform time step size we take $\tau = h_0^2$, where h_0 denotes the maximal element diameter of Γ^0. Of course, for the last time step we use the time step size $T - t_{M-1} = T - (M-1)\,\tau$. We observe that both schemes show very similar errors, indicating a convergence order of at least $\mathcal{O}(h_0^2)$.

4.2 Numerical simulations in 2d

In this section we consider some numerical simulations for two-phase flow with insoluble surfactant in two space dimensions. We begin with a comparison between the schemes

h_0	(3.42c,e)	(3.48c–e)
3.9018e-01	5.9569e-03	6.1760e-03
1.9603e-01	2.4356e-04	2.4544e-04
9.8135e-02	2.1006e-04	2.1197e-04
4.9082e-02	9.0700e-06	9.1626e-06
2.4543e-02	1.3328e-06	1.3469e-06

Table 1: The errors $\|\Psi - \psi\|_{L^2}$ for the convergence experiment for $d = 2$.

h_0	(3.42c,e)	(3.48c–e)
7.6537e-01	3.1233e-02	1.7760e-02
4.0994e-01	2.6612e-03	3.1695e-03
2.0854e-01	4.1570e-04	4.2492e-04
1.0472e-01	2.1768e-05	2.1966e-05
5.2416e-02	6.0305e-06	6.0785e-06

Table 2: The errors $\|\Psi - \psi\|_{L^2}$ for the convergence experiment for $d = 3$.

(3.42a–e) and (3.48a–e) for a rising bubble experiment that is motivated by the benchmark problems in Hysing *et al.* (2009) for two-phase Navier–Stokes flow.

4.2.1 Rising bubble benchmark problem 1

We use the setup described in Hysing *et al.* (2009), see Figure 2 there; i.e. $\Omega = (0,1)\times(0,2)$ with $\partial_1\Omega = [0,1] \times \{0,2\}$ and $\partial_2\Omega = \{0,1\} \times (0,2)$. Moreover, $\Gamma_0 = \{\vec{z} \in \mathbb{R}^2 : |\vec{z} - (\frac{1}{2},\frac{1}{2})^T| = \frac{1}{4}\}$. The physical parameters from the test case 1 in Hysing *et al.* (2009, Table I), in the absence of surfactant, are given by

$$\rho_+ = 1000\,, \quad \rho_- = 100\,, \quad \mu_+ = 10\,, \quad \mu_- = 1\,, \quad \gamma_0 = 24.5\,, \quad \vec{f}_1 = -0.98\,\vec{e}_d\,, \quad \vec{f}_2 = \vec{0}\,, \tag{4.1}$$

where, here and throughout, $\{\vec{e}_j\}_{j=1}^d$ denotes the standard basis in $\mathbb{R}^d$. The time interval chosen for the simulation is $[0,T]$ with $T = 3$. For the surfactant problem we choose the parameters $\mathcal{D}_\Gamma = 0.1$ and (2.14a) with $\beta = 0.5$.

We start with a simulation for the scheme (3.42a–e), using the discretization parameters $\text{adapt}_{7,3}$. The results can be seen on the left of Figure 2. Two things are immediately evident. Firstly, the area of the inner phase is not conserved. In fact, in this computation the relative area loss for the inner phase is 62%. And secondly, we see that the vertices of the approximation Γ^m are transported, similarly to the surfactant, with the fluid flow. This means that many vertices can be found at the bottom of the bubble, with hardly any vertices left at the top. The second behaviour can be improved by allowing local mesh refinements on Γ^m, recall Remark 3.13. In particular, we refine an element σ^m on Γ^m whenever $\mathcal{H}^{d-1}(\sigma^m) > \frac{7}{4} \max_{j=1,\dots,J_\Gamma} \mathcal{H}^{d-1}(\sigma_j^0)$. Then the interface remains well resolved,

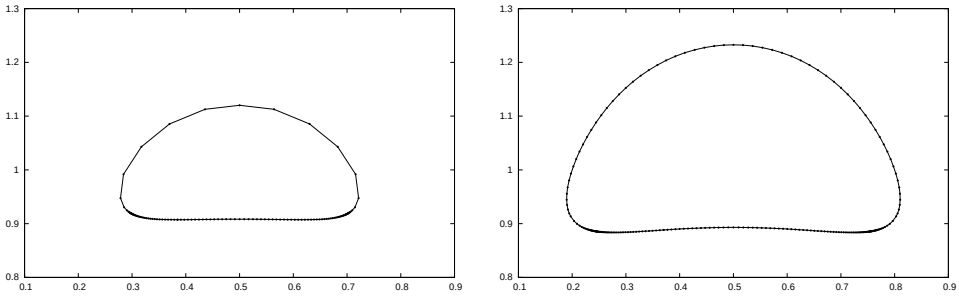

Figure 2: (adapt$_{7,3}$) Vertex distributions for the final bubbles for the benchmark problem 1 at time $T = 3$ for the scheme (3.42a–e) without local refinement on Γ^m (left), and with local refinement (right).

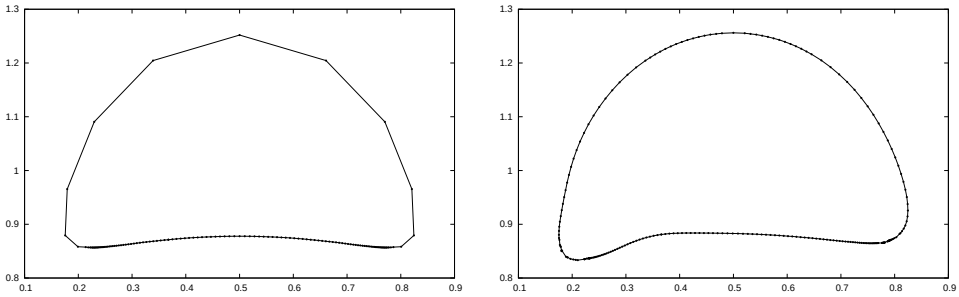

Figure 3: (adapt$_{7,3}$) Vertex distributions for the final bubbles for the benchmark problem 1 at time $T = 3$ for a variant of the scheme (3.42a–e) without local refinement on Γ^m (left) and with local refinement (right). The loss of symmetry is caused by coalescence of vertices.

and the final number of elements is $J_\Gamma^M = 252 > 128 = J_\Gamma^0$. However, coalescence of vertices can still be observed at the bottom of the bubble, see the plot on the right of Figure 2. We remark that for the latter computation the area of the inner phase decreases by 14%. For completeness we note that this dramatic area loss is connected to mass lumping being employed on the right hand side of (3.42c). To visualize this effect, we repeat the above computations now for $\langle \vec{U}^{m+1}, \vec{\chi} \rangle_{\Gamma^m}^h$ in (3.42c) replaced by $\langle \vec{U}^{m+1}, \vec{\chi} \rangle_{\Gamma^m}$. The semidiscrete variant of this new approximation then no longer satisfies the stability result in Theorem 3.3. However, in practice this approximation appears to perform much better, with the relative area loss of the inner phase now down to 1.4% for the simulation without local refinement. The simulation with local refinement leads to coalescence of vertices and a clear loss of symmetry, which is of course unphysical, see Figure 3.

The same computation for our preferred scheme (3.48a–e), where no local refinements need to be performed because the tangential movement of vertices yields an almost equidistributed approximation of Γ^m, can be seen in Figure 4, where we compare the run with $\beta = 0.5$ also to the case of constant surface tension, i.e. $\beta = 0$. We remark that for these computations the areas of the two phases, as well as the total surfactant mass on Γ^m,

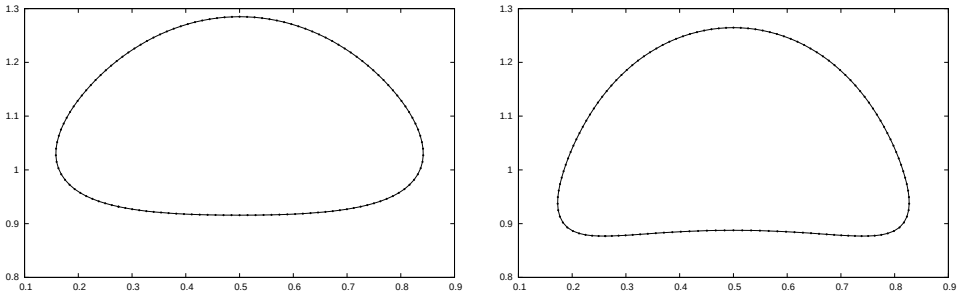

Figure 4: (adapt$_{7,3}$) Vertex distributions for the final bubble for the benchmark problem 1 at time $T = 3$ for the scheme (3.48a–e). On the left the computation with $\beta = 0$, on the right with $\beta = 0.5$.

were conserved.

In Figure 5 we show the surfactant concentrations Ψ^M on the final bubble for the two schemes (3.42a–e) and (3.48a–e), where in the computation for the former scheme we employ local mesh refinements. We observe that the numerical results are in rough agreement, apart from the smaller bubble for the scheme (3.42a–e) because of the loss of area for the inner phase. We also show a plot of the discrete surface energy $\langle F(\Psi^m), 1\rangle^h_{\Gamma^m}$, where for (3.48a–e) it holds that $\langle F_\varepsilon(\Psi^m), 1\rangle^h_{\Gamma^m} = \langle F(\Psi^m), 1\rangle^h_{\Gamma^m}$ throughout the evolution. Here it can be seen that the plots for the two approximations differ significantly, most probably because of the area loss for the scheme (3.42a–e).

The poor mesh properties of the scheme (3.42a–e), together with the fact that the volume of the two phases is in general not conserved, mean that this scheme is not very practical. Of course, the same applies to the scheme from Remark 3.9. It is for this reason that from now on we only consider numerical experiments for the scheme (3.48a–e).

The parameters in (4.1) were proposed in Hysing *et al.* (2009, Table I) in order to define a test case for two-phase flow, in the absence of surfactant, for which benchmark computations can be performed. We now report on these benchmark quantities also in the presence of surfactant. To this end, we recall from Barrett *et al.* (2013b) our fully discrete approximations for the x_2-component of the bubble's centre of mass, the bubble's "degree of circularity" and the rise velocity:

$$y_c^m = \frac{1}{\mathcal{L}^2(\Omega_-^m)} \int_{\Omega_-^m} x_2 \,\mathrm{d}\mathcal{L}^2\,, \quad \mathscr{C}^m = 2\,[\pi\,\mathcal{L}^2(\Omega_-^m)]^{\frac{1}{2}}\,[\mathcal{H}^1(\Gamma^m)]^{-1}\,, \quad V_c^m = \frac{(\rho_-^m\,\vec{U}^m, \vec{e}_d)}{(\rho_-^m, 1)}\,, \tag{4.2}$$

where $\rho_-^m \in S_0^m$ is defined as in (3.41) but with ρ_+ replaced by zero. Finally, we also define the relative overall area/volume loss as

$$\mathcal{L}_{\text{loss}} = \frac{\mathcal{L}^d(\Omega_-^0) - \mathcal{L}^d(\Omega_-^M)}{\mathcal{L}^d(\Omega_-^0)}\,.$$

In Table 3 we report on these quantities for simulations with and without surfactant for our preferred scheme (3.48a–e). Here we note that the numbers for the simulations

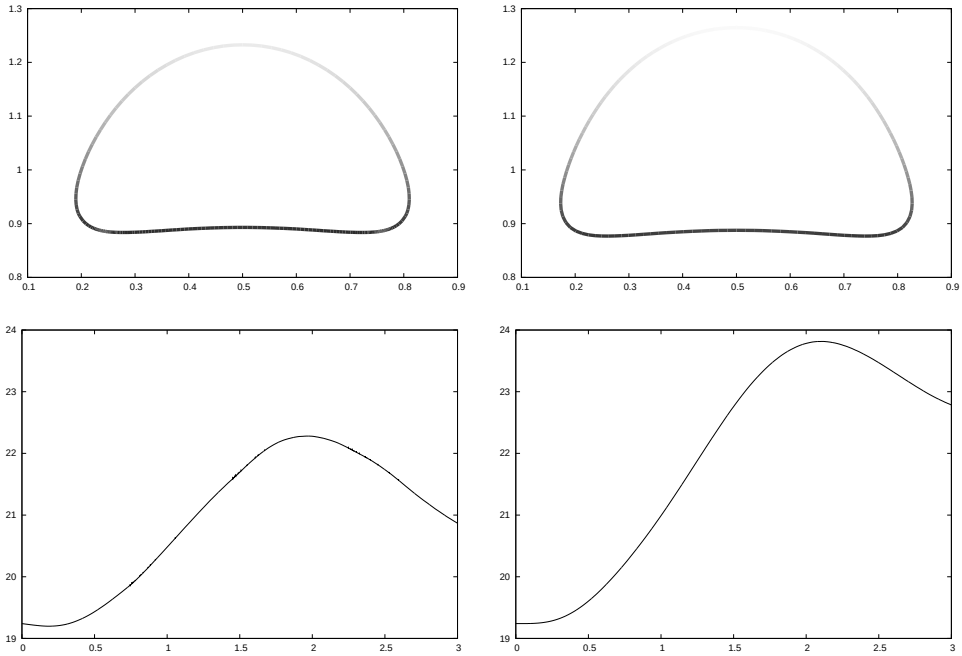

Figure 5: ($\text{adapt}_{7,3}$) The surfactant concentration on the final bubbles for the benchmark problem 1 at time $T = 3$ for the schemes (3.42a–e) and (3.48a–e). The grey scales linearly with the surfactant concentration ranging from 0.4 (white) to 1.4 (black). Below we present plots of $\langle F(\Psi^m), 1\rangle^h_{\Gamma^m}$ over time for the two schemes.

without surfactant differ slightly from the ones in Barrett *et al.* (2013b, Table 2), because the finite element approximations employed here is different, recall Remark 3.12. In what follows we present some visualizations of the numerical results for the runs with the discretization parameters $5\,\text{adapt}_{11,5}$. A plot of Γ^M can be seen in Figure 6, while the time evolution of the circularity, the centre of mass and the rise velocity are shown in Figures 7 and 8.

4.2.2 Rising bubble benchmark problem 2

In a second set of benchmark computations, we fix

$$\rho_+ = 1000\,, \quad \rho_- = 1\,, \quad \mu_+ = 10\,, \quad \mu_- = 0.1\,, \quad \gamma_0 = 1.96\,, \quad \vec{f}_1 = -0.98\,\vec{e}_d\,, \quad \vec{f}_2 = \vec{0}\,, \tag{4.3}$$

as in test case 2 in Hysing *et al.* (2009, Table I). For the surfactant problem we again let $\mathcal{D}_\Gamma = 0.1$ and let $\beta = 0.5$ in (2.14a). In Table 4 we report on some benchmark quantities for simulations with and without surfactant for our preferred scheme (3.48a–e). Here we note that in contrast to the experiments in §4.2.1, there is little difference between the numbers for the runs with and without surfactant. This is because in the simulations for (4.3) the large values of $\frac{\rho_+}{\rho_-}$ and $\frac{\mu_+}{\mu_-}$ dominate the evolution. In particular, they lead to elongated fingers developing at the bottom of the rising bubble which means that there is a significant growth in the overall interface length. In order to account for this growth,

	$\text{adapt}_{5,2}$	$\text{adapt}_{7,3}$	$2\,\text{adapt}_{9,4}$	$5\,\text{adapt}_{11,5}$
$\mathcal{L}_{\text{loss}}$	0.0%	0.0%	0.0%	0.0%
$\phi_{\min}$	0.9135	0.9069	0.9034	0.9022
$t_{\phi=\phi_{\min}}$	2.0760	1.9420	1.9105	1.9028
$V_{c,\max}$	0.2477	0.2415	0.2413	0.2420
$t_{V_c=V_{c,\max}}$	0.9470	0.9360	0.9255	0.9698
$y_c(t=3)$	1.0906	1.0822	1.0814	1.0815
	$\text{adapt}_{5,2}$	$\text{adapt}_{7,3}$	$2\,\text{adapt}_{9,4}$	$5\,\text{adapt}_{11,5}$
$\mathcal{L}_{\text{loss}}$	0.0%	0.0%	0.0%	0.0%
$\phi_{\min}$	0.8779	0.8715	0.8681	0.8669
$t_{\phi=\phi_{\min}}$	2.1330	2.0710	2.0550	2.0500
$V_{c,\max}$	0.2279	0.2243	0.2236	0.2237
$t_{V_c=V_{c,\max}}$	1.0070	0.9040	0.9010	0.8710
$y_c(t=3)$	1.0423	1.0449	1.0467	1.0473

Table 3: Some quantitative results for the benchmark problem 1. Without surfactant (top) and with surfactant (bottom).

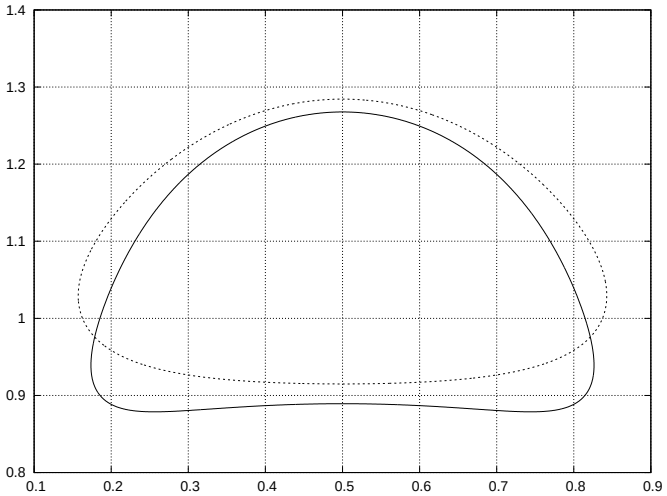

Figure 6: ($5\,\text{adapt}_{11,5}$) The final bubble with surfactant for the benchmark problem 1 at time $T = 3$. The clean bubble is shown dashed.

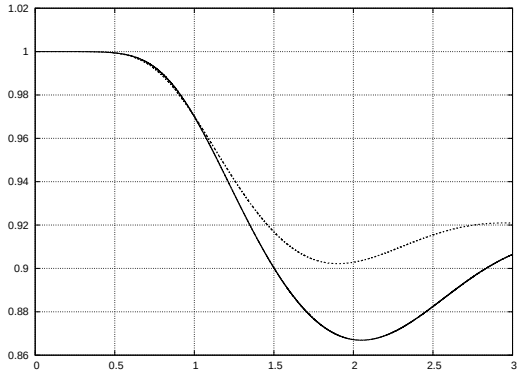

Figure 7: ($5\,\mathrm{adapt}_{11,5}$) Circularity of the surfactant bubble for the benchmark problem 1. The dashed line is for the clean bubble.

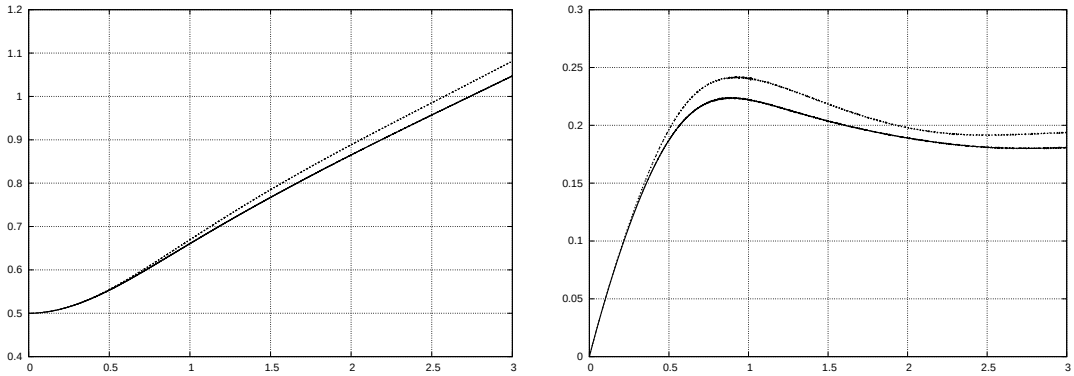

Figure 8: ($5\,\mathrm{adapt}_{11,5}$) Centre of mass and rise velocity for the surfactant bubble for the benchmark problem 1. The dashed lines are for the clean bubble.

we locally refine Γ^m in all the simulations for the parameters as in (4.3). Here, similarly to the experiment on the right of Figure 2, we refine an element σ^m on Γ^m whenever $\mathcal{H}^{d-1}(\sigma^m) > \frac{7}{4} \max_{j=1,\dots,J_\Gamma} \mathcal{H}^{d-1}(\sigma_j^0)$. In what follows we present some visualizations of the numerical results for the runs with the discretization parameters $2\,\mathrm{adapt}_{9,4}$. A plot of Γ^M can be seen in Figure 9, where we also show the final surfactant concentration Ψ^M. Here we observe that most of the surfactant has accumulated at the inner side walls of the lower part of the bubble. It is worth pointing out that our numerical method has no difficulties in computing the evolution of the advection-diffusion equation on a highly deformed interface as seen in Figure 9. The time evolution of the circularity, the centre of mass and the rise velocity are shown in Figures 10 and 11.

4.2.3 Bubble in shear flow

In the literature on numerical methods for two-phase flow with insoluble surfactant it is often common to consider shear flow experiments for an initially circular bubble in order to study the effect of surfactants and of different equations of state. In this subsection, we will perform such simulations for our preferred scheme (3.48a–e). Here we consider

	$\text{adapt}_{5,2}$	$\text{adapt}_{7,3}$	$2\,\text{adapt}_{9,4}$
$\mathcal{L}_{\text{loss}}$	0.0%	0.0%	0.0%
$\phi_{\min}$	0.5890	0.5198	0.5165
$t_{\phi=\phi_{\min}}$	3.0000	3.0000	3.0000
$V_{c,\max 1}$	0.2584	0.2480	0.2489
$t_{V_c=V_{c,\max 1}}$	0.8800	0.7610	0.7295
$V_{c,\max 2}$	0.2283	0.2305	0.2357
$t_{V_c=V_{c,\max 2}}$	2.0000	1.9510	2.0485
$y_c(t=3)$	1.1275	1.1239	1.1319
	$\text{adapt}_{5,2}$	$\text{adapt}_{7,3}$	$2\,\text{adapt}_{9,4}$
$\mathcal{L}_{\text{loss}}$	0.0%	0.0%	0.0%
$\phi_{\min}$	0.5449	0.4996	0.4891
$t_{\phi=\phi_{\min}}$	3.0000	3.0000	3.0000
$V_{c,\max 1}$	0.2565	0.2467	0.2476
$t_{V_c=V_{c,\max 1}}$	0.8830	0.7370	0.7395
$V_{c,\max 2}$	0.2283	0.2326	0.2391
$t_{V_c=V_{c,\max 2}}$	2.0070	2.0330	2.0830
$y_c(t=3)$	1.1217	1.1197	1.1294

Table 4: Some quantitative results for the benchmark problem 2. Without surfactant (top) and with surfactant (bottom).

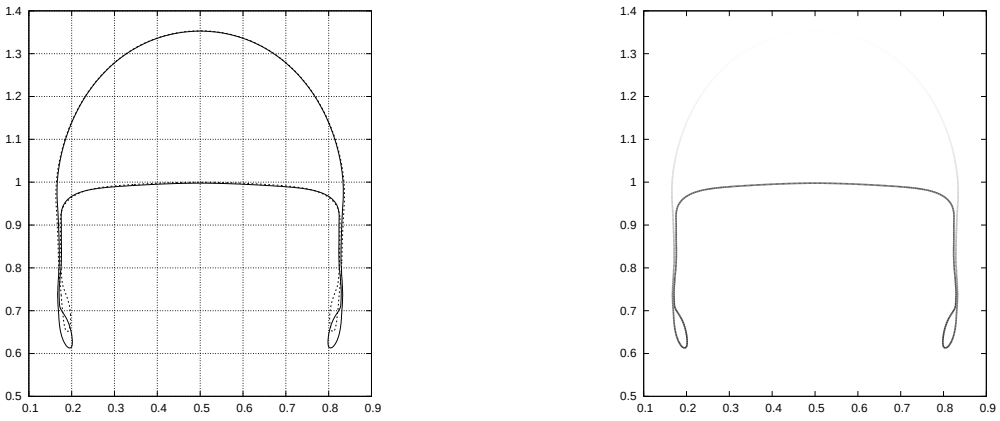

Figure 9: ($2\,\text{adapt}_{9,4}$) The final bubble with surfactant for the benchmark problem 2 at time $T = 3$, with the surfactant concentration on the right. The grey scales linearly with the surfactant concentration ranging from 0.1 (white) to 0.9 (black). The dashed curve on the left represents the final shape of the clean bubble.

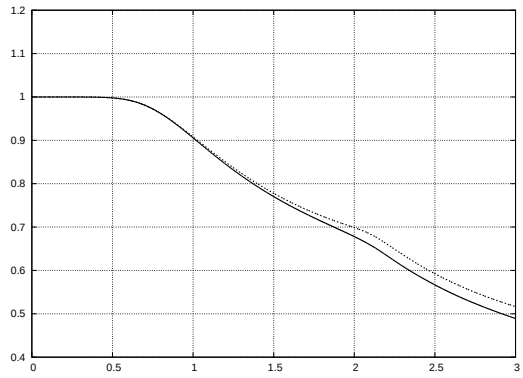

Figure 10: ($2\,\mathrm{adapt}_{9,4}$) Circularity of the surfactant bubble for the benchmark problem 2. The dashed line is for the clean bubble.

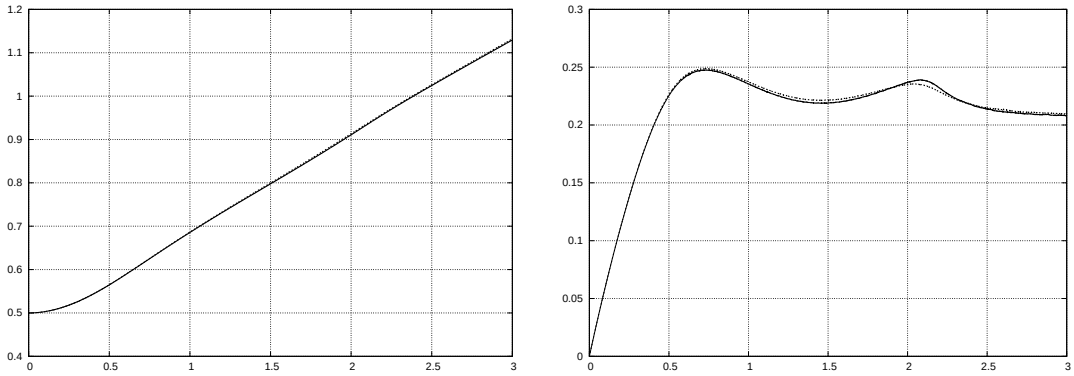

Figure 11: ($2\,\mathrm{adapt}_{9,4}$) Centre of mass and rise velocity for the surfactant bubble for the benchmark problem 2. The dashed lines are for the clean bubble.

the setup from Lai *et al.* (2008, Fig. 1). In particular, we let $\Omega = (-5,5) \times (-2,2)$ and prescribe the inhomogeneous Dirichlet boundary condition $\vec{g}(\vec{z}) = (\frac{1}{2}\, z_2, 0)^T$ on $\partial\Omega = \partial_1\Omega$. Moreover, $\Gamma_0 = \{\vec{z} \in \mathbb{R}^2 : |\vec{z}| = 1\}$. The physical parameters are given by

$$\rho_+ = \rho_- = 1\,, \quad \mu_+ = \mu_- = 0.1\,, \quad \gamma_0 = 0.2\,, \quad \mathcal{D}_\Gamma = 0.1\,, \quad \vec{f} = \vec{0}\,, \quad \vec{u}_0 = \vec{g}\,. \tag{4.4}$$

First we compare the evolutions for the linear equation of state (2.14a) for (i) $\beta = 0$, (ii) $\beta = 0.25$ and (iii) $\beta = 0.5$. Our numerical results appear to agree very well with the ones in Lai *et al.* (2008, Fig. 1); see Figure 12 for more details. On recalling (4.2), we note that the "circularities" ϕ^M of the final bubbles are given by 0.68, 0.59 and 0.51, respectively. Moreover, we remark that for these simulations the relative overall area loss satisfies $|\mathcal{L}_{\mathrm{loss}}| < 0.02\%$, and the same holds true for all of the remaining numerical experiments in this subsection.

In the next experiment we choose the nonlinear equation of state (2.14b) with $\psi_\infty = \frac{1}{\beta}$; see also Lai *et al.* (2008, Fig. 6). We show the evolutions of the drop for $\beta = 0.25$ and for $\beta = 0.5$ in Figure 13. A detailed comparison of the final drop shapes for the two equations of state (2.14a,b) can be seen in Figure 14. As expected, the difference between the simulations for the two equations of state are more pronounced for the larger value

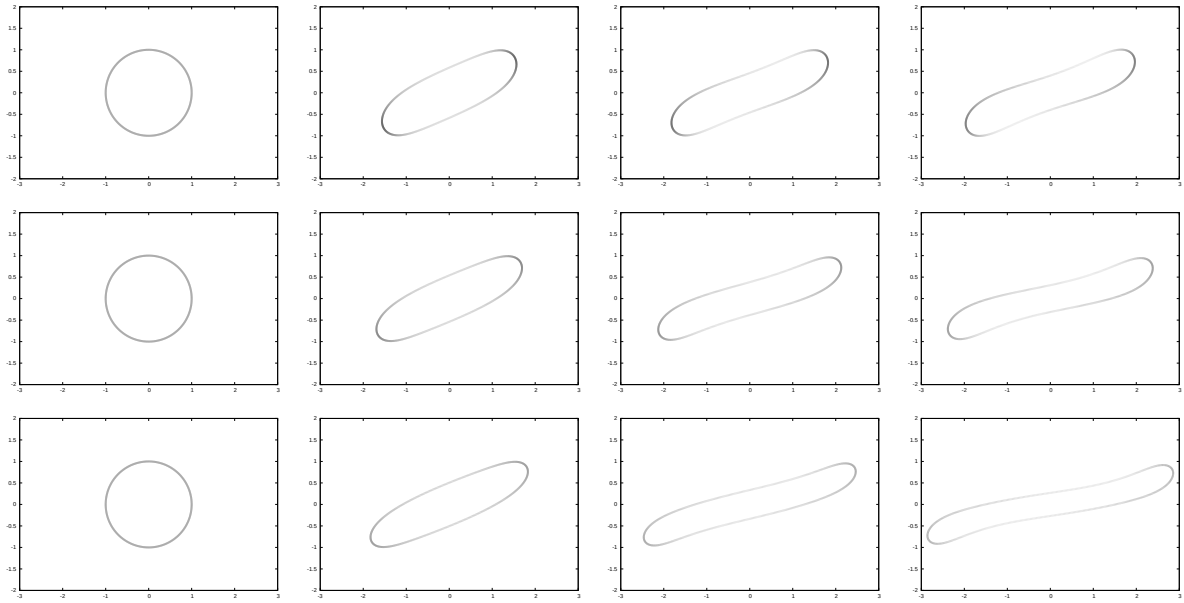

Figure 12: ($2\,\text{adapt}_{9,4}$) The time evolution of a drop in shear flow for (2.14a) with $\beta = 0$ (top), $\beta = 0.25$ (middle) and $\beta = 0.5$ (bottom). Plots are at times $t = 0$, 4, 8, 12. The grey scales linearly with the surfactant concentration ranging from 0.2 (white) to 1.6 (black).

of β.

In Figure 15 we compare the previously used (2.14a) with $\beta = 0.5$ and (2.14b) with $\psi_\infty^{-1} = \beta = 0.5$ to (2.14b) with $\beta = 0.5$ and $\psi_\infty = 1.3$. This indicates that the initial drop should now be more unstable. However, the evolution is not very different to what we saw before, see Figure 16. This is despite the maximum discrete surfactant concentration being ≈ 1.08, which means that the discrete surface tension $\gamma(\Psi^m)$ at times is negative. In fact, the observed minimum value is < -0.03, compare with Figure 15, but this posed no problem for our numerical method.

On returning back to the linear equation of state (2.14a), we also present a numerical simulation for different densities and viscosities. In particular, we leave all the parameters as in (4.4), but now choose

$$\rho_+ = 10\,, \quad \rho_- = 1\,, \quad \mu_+ = 1\,, \quad \mu_- = 0.1\,.$$

We show the evolution of the drop in Figure 17 for $\beta = 0$, 0.25 and 0.5. In contrast to Figure 12, the presence of surfactant has very little impact on the shape of the drop here. However, the interfaces in Figure 17 are more distorted and have higher curvatures at the ends, which is a well-known fact when the viscosity of the drop is much less than the one of the surrounding fluid, see Renardy *et al.* (2002).

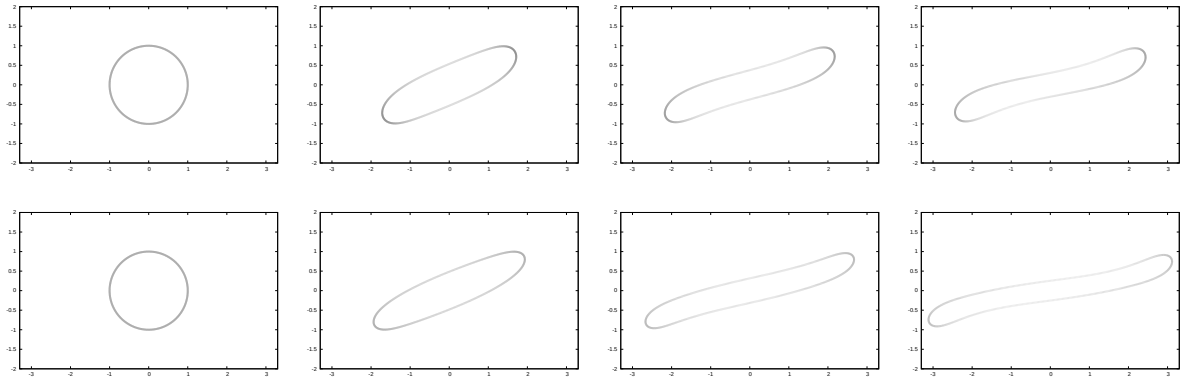

Figure 13: ($2\,\mathrm{adapt}_{9,4}$) The time evolution of a drop in shear flow for (2.14b) with $\beta = 0.25$ (top) and $\beta = 0.5$ (bottom). Plots are at times $t = 0$, 4, 8, 12. The grey scales linearly with the surfactant concentration ranging from 0.2 (white) to 1.6 (black).

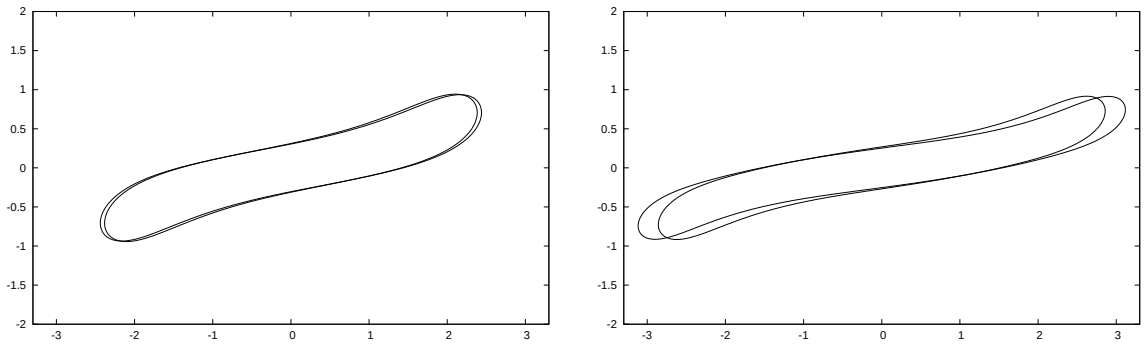

Figure 14: ($2\,\mathrm{adapt}_{9,4}$) Comparison of the final drop shapes in shear flow for a linear (2.14a) and a nonlinear (2.14b) equation of state with $\beta = 0.25$ (left) and $\beta = 0.5$ (right). In each case the shape for (2.14b) is more elongated.

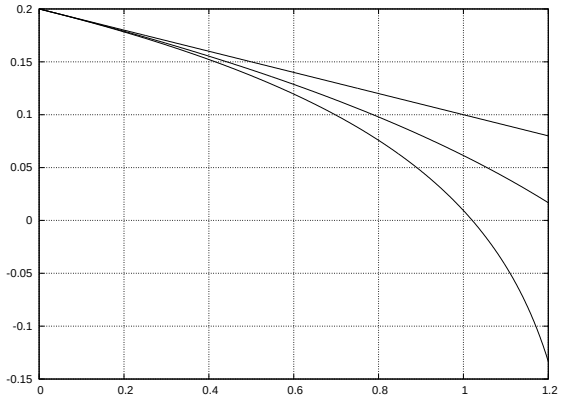

Figure 15: ($\beta = 0.5$) Plots of $\gamma(r)$ for the linear equation of state (2.14a) and the nonlinear equation of state (2.14b) with $\psi_\infty = 2$ and 1.3.

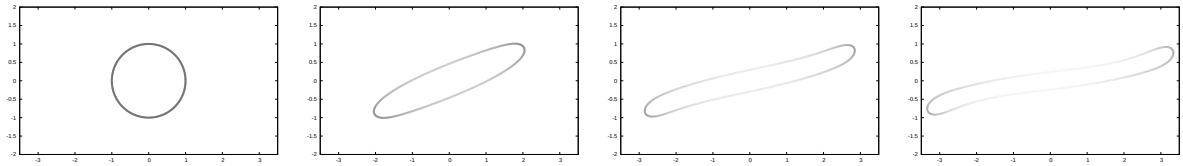

Figure 16: ($2\,\mathrm{adapt}_{9,4}$) The time evolution of a drop in shear flow for (2.14b) with $\beta = 0.5$ and $\psi_\infty = 1.3$. Plots are at times $t = 0$, 4, 8, 12. The grey scales linearly with the surfactant concentration ranging from 0.3 (white) to 1.1 (black).

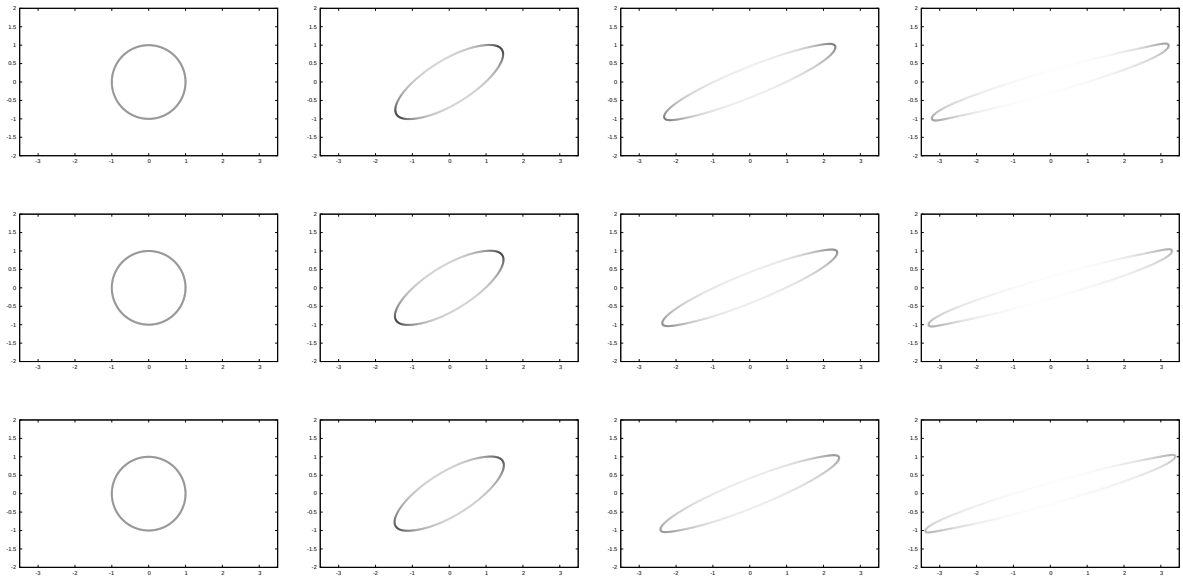

Figure 17: ($2\,\mathrm{adapt}_{9,4}$) The time evolution of a drop in shear flow for (2.14a) with $\beta = 0$ (top), $\beta = 0.25$ (middle) and $\beta = 0.5$ (bottom). Here $\rho_+ = 10$, $\rho_- = 1$, $\mu_+ = 1$, $\mu_- = 0.1$. Plots are at times $t = 0$, 2, 4, 6. The grey scales linearly with the surfactant concentration ranging from 0.3 (white) to 1.3 (black).

4.3 Numerical simulations in 3d

In this section we consider some numerical simulations for two-phase flow with insoluble surfactant in three space dimensions. Here we will always report on simulations for our preferred scheme (3.48a–e).

4.3.1 Rising bubble benchmark problem 1

Here we consider the natural 3d analogue of the problem in §4.2.1. To this end, we let $\Omega = (0,1)\times(0,1)\times(0.2)$ with $\partial_1\Omega = [0,1]\times[0,1]\times\{0,2\}$ and $\partial_2\Omega = \partial\Omega\setminus\partial_1\Omega$. Moreover, we set $T = 3$, $\Gamma_0 = \{\vec{z}\in\mathbb{R}^3 : |\vec{z} - (\frac{1}{2},\frac{1}{2},\frac{1}{2})^T| = \frac{1}{4}\}$, and choose the physical parameters as in (4.1). The time interval chosen for the simulation is again $[0,T]$ with $T = 3$. For the

	$\text{adapt}_{5,2}$	$\text{adapt}_{6,3}$
$\mathcal{L}_{\text{loss}}$	0.0%	0.0%
$\not{\Phi}_{\min}$	0.9570	0.9508
$t_{\not{\Phi}=\not{\Phi}_{\min}}$	3.0000	3.0000
$V_{c,\max}$	0.3822	0.3845
$t_{V_c=V_{c,\max}}$	1.1930	1.0790
$z_c(t=3)$	1.5515	1.5555

	$\text{adapt}_{5,2}$	$\text{adapt}_{6,3}$
$\mathcal{L}_{\text{loss}}$	0.0%	0.0%
$\not{\Phi}_{\min}$	0.9348	0.9297
$t_{\not{\Phi}=\not{\Phi}_{\min}}$	2.9300	2.9970
$V_{c,\max}$	0.3252	0.3296
$t_{V_c=V_{c,\max}}$	0.8160	0.8960
$z_c(t=3)$	1.3807	1.3902

Table 5: Some quantitative results for the 3d benchmark problem 1. Without surfactant (left) and with surfactant (right).

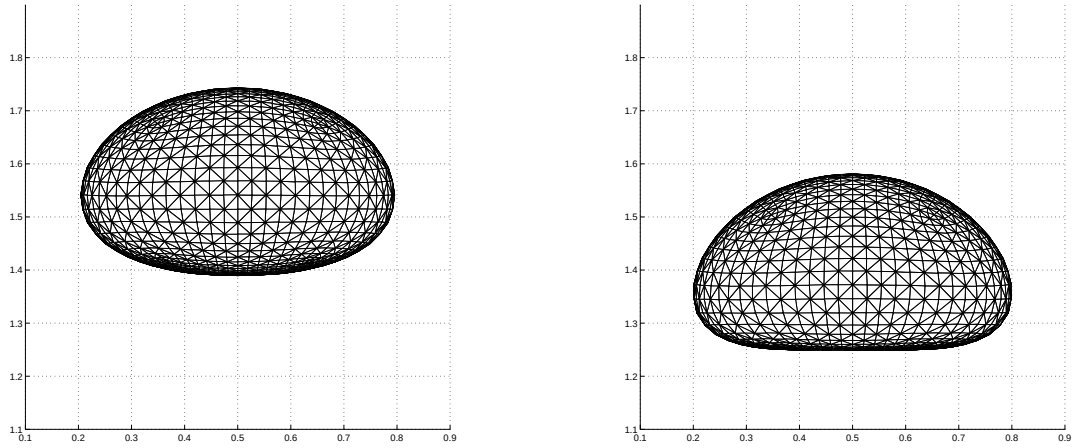

Figure 18: ($\text{adapt}_{6,3}$) Side view of the final bubble for the 3d benchmark problem 1 at time $T = 3$. Without surfactant (left) and with surfactant (right).

surfactant problem we choose the parameters $\mathcal{D}_\Gamma = 0.1$ and (2.14a) with $\beta = 0.5$.

Some quantitative values for the evolution are given in Table 5, where we have introduced the natural extensions of the quantities defined in (4.2). In particular, the discrete approximations of the x_3-component of the bubble's centre of mass and the "degree of sphericity" are defined by

$$z_c^m = \frac{1}{\mathcal{L}^3(\Omega_-^m)} \int_{\Omega_-^m} x_3 \,\mathrm{d}\mathcal{L}^3 = \frac{3}{\int_{\Gamma^m} \vec{X}^m \,.\, \vec{\nu}^m \,\mathrm{d}\mathcal{H}^2} \int_{\Gamma^m} \tfrac{1}{2} \,(\vec{X}^m \,.\, \vec{e}_3)^2 \,(\vec{\nu}^m \,.\, \vec{e}_3) \,\mathrm{d}\mathcal{H}^2 \,,$$
$$\not{\Phi}^m = \pi^{\frac{1}{3}} \,[6\,\mathcal{L}^3(\Omega_-^m)]^{\frac{2}{3}} \,[\mathcal{H}^2(\Gamma^m)]^{-1} \,.$$

In what follows we present some visualizations of the numerical results for the runs with $\text{adapt}_{6,3}$. A comparison of the final meshes for the runs with and without surfactant can be seen in Figure 18, while the discrete surfactant concentration for the run with surfactant can be seen in Figure 19.

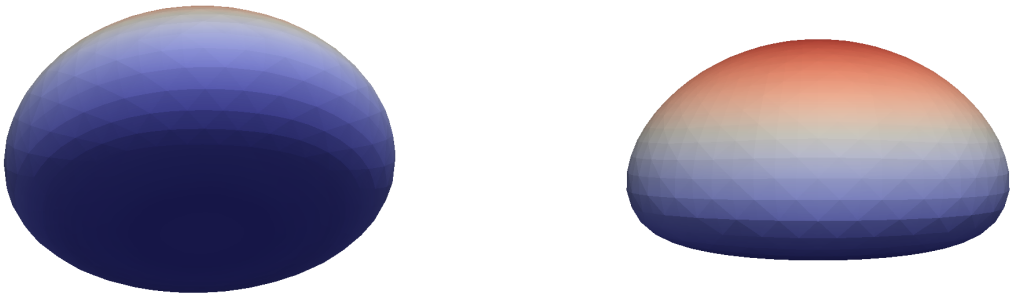

Figure 19: ($\text{adapt}_{6,3}$) The final surfactant concentration Ψ^M on Γ^M. Here the colour ranges from red (0.5) to blue (1.2).

4.3.2 Bubble in shear flow

In this subsection we report on the 3d analogues of the computations shown in Figure 12. In particular, in Figure 20 we show shear flow experiments on the domain $\Omega = (-5,5) \times (-2,2)^2$ with $\partial\Omega = \partial_1\Omega$ and $\vec{g}(\vec{z}) = (\frac{1}{2}\, z_3, 0, 0)^T$. The physical parameters are as in (4.4), and we compare the evolutions for the linear equation of state (2.14a) for (i) $\beta = 0$, (ii) $\beta = 0.25$ and (iii) $\beta = 0.5$. As the discretization parameters we choose $\text{adapt}^\star_{5,2}$, which are the same as for $\text{adapt}_{5,2}$, apart from $\tau = 0.01$ and $(K_\Gamma, J_\Gamma) = (1538, 3072)$, i.e. $\text{adapt}^\star_{5,2}$ uses a larger time step size and a finer interface mesh compared to $\text{adapt}_{5,2}$. Our three dimensional results turn out to be very similar to the two dimensional results in Figure 12; see Figure 20 for more details.

A Exact solution for the advection diffusion equation

Following Dziuk and Elliott (2007, Example 7.3), we present a true solution to the inhomogeneous advection diffusion equation

$$\partial_t^\bullet\, \psi + \psi\, \nabla_s . \vec{u} - \Delta_s\, \psi = f_\Gamma \qquad \text{on } \Gamma(t)\,, \tag{A.1}$$

recall (2.9), in a situation where the fluid velocity $\vec{u}$, and hence the evolution of $\Gamma(t)$, is given. The surface is given by $\Gamma(t) = \{\vec{z} \in \mathbb{R}^d : \phi(\vec{z}, t) = 1\}$, where

$$\phi(\vec{z}, t) = [a(t)]^{-1}\, z_1^2 + \sum_{i=2}^{d} z_i^2\,,$$

so that the moving surface $\Gamma(t)$ is an ellipsoid with time dependent x_1-axis. Here we choose

$$a(t) = 1 + \sin(\pi\, t)\,,$$

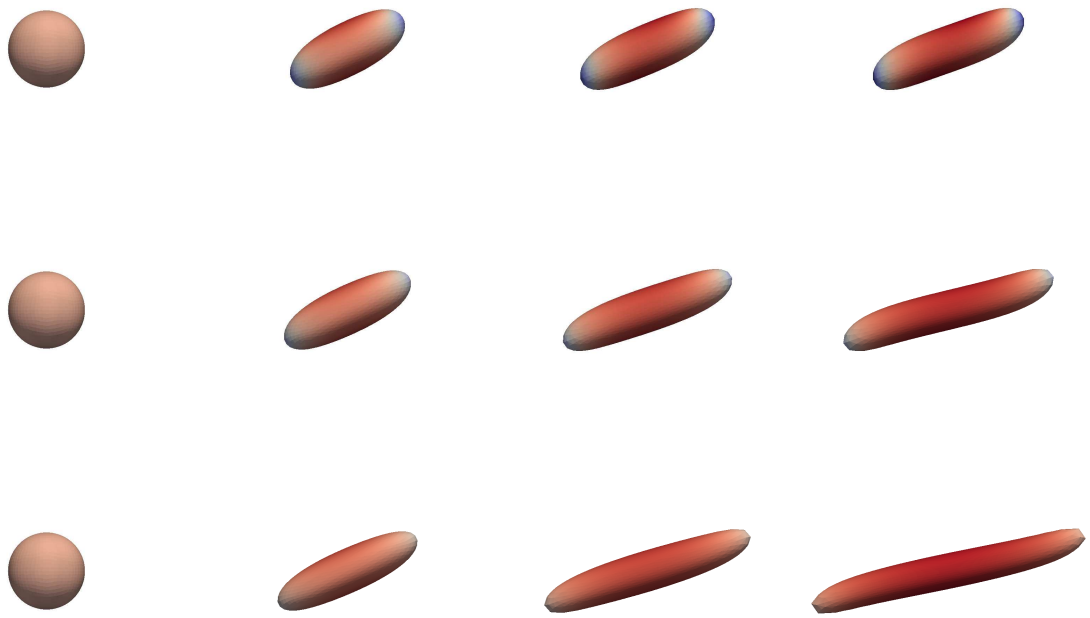

Figure 20: (adapt$^\star_{5,2}$) The discrete surfactant concentrations Ψ^m at times $t = 0, 4, 8, 12$ for $\beta = 0$ (top), $\beta = 0.25$ (middle) and $\beta = 0.5$ (bottom). The colour ranges from red (0.5) to blue (1.9).

and as the parameterization $\vec{x}(\cdot, t) : \mathbb{S}^{d-1} \to \Gamma(t)$, where $\mathbb{S}^{d-1} := \{\vec{q} \in \mathbb{R}^d : |\vec{q}| = 1\}$, we choose

$$\vec{x}(\vec{q}, t) = [a(t)]^{\frac{1}{2}}\, q_1\, \vec{e}_1 + \sum_{i=2}^{d} q_i\, \vec{e}_i \qquad \forall\ \vec{q} \in \mathbb{S}^{d-1}\,, \quad t \in \mathbb{R}_{\geq 0}\,.$$

On recalling (2.2), for the fluid velocity we naturally choose

$$\vec{u}(\vec{z}, t) = \tfrac{1}{2}\, [a(t)]^{-1}\, a'(t)\, z_1\, \vec{e}_1 \qquad \vec{z} \in \Omega\,, \tag{A.2}$$

so that

$$\vec{u}(\vec{z}, t)\,|_{\Gamma(t)} = \vec{\mathcal{V}}(\vec{z}, t) \qquad \vec{z} \in \Gamma(t)\,.$$

As an exact solution we choose $\psi(\vec{z}, t) = e^{-6\,t}\, z_1\, z_2$, and hence it remains to calculate the right hand side f_Γ in (A.1) for our chosen ψ and $\vec{u}$. To this end we note that

$$f_\Gamma = \partial_t^\bullet\, \psi + \psi\, \nabla_s\,.\vec{u} - \Delta_s\, \psi\,, \tag{A.3}$$

with

$$\begin{aligned}
\partial_t^\bullet\, \psi &= (\tfrac{1}{2}\, [a(t)]^{-1}\, a'(t) - 6)\, \psi\,,\\
\psi\, \nabla_s\,.\vec{u} &= \tfrac{1}{2}\, [a(t)]^{-1}\, a'(t)\, (1 - \nu_1^2)\, \psi\,,\\
-\Delta_s\, \psi(\vec{z}, t) &= e^{-6\,t}\, [2\, \nu_1\, \nu_2 - (\nu_1\, z_2 + \nu_2\, z_1)\, \varkappa(\vec{z}, t)]\,,
\end{aligned}$$

where $\vec{\nu}(\vec{z},t) = \frac{\nabla\phi(\vec{z},t)}{|\nabla\phi(\vec{z},t|} \in \mathbb{R}^d$ denotes the normal to $\Gamma(t)$ at $\vec{z} \in \Gamma(t)$, and where

$$\varkappa = -\nabla_s \,.\, \vec{\nu} = -\nabla \,.\, \vec{\nu} = -|\nabla\,\phi|^{-1} \sum_{i=1}^{d} \left[\left(1 - |\nabla\,\phi|^{-2} \left(\frac{\partial \phi}{\partial z_i} \right)^2 \right) \frac{\partial^2 \phi}{\partial z_i^2} \right] \tag{A.4}$$

denotes the mean curvature of $\Gamma(t)$. Of course, for our example we have that $\nabla\,\phi(\vec{z},t) = 2\,[a(t)]^{-1}\,z_1\,\vec{e}_1 + 2\sum_{i=2}^{d} z_i\,\vec{e}_i$, and so (A.4) reduces to

$$\varkappa = -2\,|\nabla\,\phi|^{-1}\,[a(t)]^{-1}\,\left(1 - 4\,|\nabla\,\phi|^{-2}\,[a(t)]^{-2}\,z_1^2\right) - 2\,|\nabla\,\phi|^{-1} \sum_{i=2}^{d} \left(1 - 4\,|\nabla\,\phi|^{-2}\,z_i^2\right).$$

References

Alke, A. and Bothe, D. (2009). 3D numerical modeling of soluble surfactant at fluidic interfaces based on the volume-of-fluid method. *FDMP Fluid Dyn. Mater. Process.*, **5**(4), 345–372.

Bänsch, E. (2001). Finite element discretization of the Navier–Stokes equations with a free capillary surface. *Numer. Math.*, **88**(2), 203–235.

Barrett, J. W. and Nürnberg, R. (2004). Convergence of a finite-element approximation of surfactant spreading on a thin film in the presence of van der Waals forces. *IMA J. Numer. Anal.*, **24**(2), 323–363.

Barrett, J. W., Garcke, H., and Nürnberg, R. (2003). Finite element approximation of surfactant spreading on a thin film. *SIAM J. Numer. Anal.*, **41**(4), 1427–1464.

Barrett, J. W., Garcke, H., and Nürnberg, R. (2007). A parametric finite element method for fourth order geometric evolution equations. *J. Comput. Phys.*, **222**(1), 441–462.

Barrett, J. W., Garcke, H., and Nürnberg, R. (2008). On the parametric finite element approximation of evolving hypersurfaces in $\mathbb{R}^3$. *J. Comput. Phys.*, **227**(9), 4281–4307.

Barrett, J. W., Garcke, H., and Nürnberg, R. (2010). On stable parametric finite element methods for the Stefan problem and the Mullins–Sekerka problem with applications to dendritic growth. *J. Comput. Phys.*, **229**(18), 6270–6299.

Barrett, J. W., Garcke, H., and Nürnberg, R. (2013a). Eliminating spurious velocities with a stable approximation of viscous incompressible two-phase Stokes flow. *Comput. Methods Appl. Mech. Engrg.*, **267**, 511–530.

Barrett, J. W., Garcke, H., and Nürnberg, R. (2013b). A stable parametric finite element discretization of two-phase Navier–Stokes flow. `http://arxiv.org/abs/1308.3335`.

Bäumler, K. and Bänsch, E. (2013). A subspace projection method for the implementation of interface conditions in a single-drop flow problem. *J. Comput. Phys.*, **252**, 438–457.

Bothe, D. and Prüss, J. (2010). Stability of equilibria for two-phase flows with soluble surfactant. *Quart. J. Mech. Appl. Math.*, **63**(2), 177–199.

Bothe, D., Prüss, J., and Simonett, G. (2005). Well-posedness of a two-phase flow with soluble surfactant. In *Nonlinear elliptic and parabolic problems*, volume 64 of *Progr. Nonlinear Differential Equations Appl.*, pages 37–61. Birkhäuser, Basel.

Bothe, D., Köhne, M., and Prüss, J. (2012). On two-phase flows with soluble surfactant. `http://arxiv.org/abs/1210.8131`.

Deckelnick, K., Dziuk, G., and Elliott, C. M. (2005). Computation of geometric partial differential equations and mean curvature flow. *Acta Numer.*, **14**, 139–232.

Drumright-Clarke, M. A. and Renardy, Y. (2004). The effect of insoluble surfactant at dilute concentration on drop breakup under shear with inertia. *Phys. Fluids*, **16**(1), 14–21.

Dziuk, G. (1991). An algorithm for evolutionary surfaces. *Numer. Math.*, **58**(6), 603–611.

Dziuk, G. and Elliott, C. M. (2007). Finite elements on evolving surfaces. *IMA J. Numer. Anal.*, **27**(2), 262–292.

Dziuk, G. and Elliott, C. M. (2013). Finite element methods for surface PDEs. *Acta Numer.*, **22**, 289–396.

Elliott, C. M. and Styles, V. (2012). An ALE ESFEM for solving PDEs on evolving surfaces. *Milan J. Math.*, **80**(2), 469–501.

Elliott, C. M., Stinner, B., Styles, V., and Welford, R. (2011). Numerical computation of advection and diffusion on evolving diffuse interfaces. *IMA J. Numer. Anal.*, **31**(3), 786–812.

Engblom, S., Do-Quang, M., Amberg, G., and Tornberg, A.-K. (2013). On diffuse interface modeling and simulation of surfactants in two-phase fluid flow. *Commun. Comput. Phys.*, **14**(4), 879–915.

Ganesan, S. and Tobiska, L. (2009). A coupled arbitrary Lagrangian–Eulerian and Lagrangian method for computation of free surface flows with insoluble surfactants. *J. Comput. Phys.*, **228**(8), 2859–2873.

Garcke, H. and Wieland, S. (2006). Surfactant spreading on thin viscous films: nonnegative solutions of a coupled degenerate system. *SIAM J. Math. Anal.*, **37**(6), 2025–2048.

Garcke, H., Lam, K. F., and Stinner, B. (2013). Diffuse interface modelling of soluble surfactants in two-phase flow. (to appear in Comm. Math. Sci., see also `http://arxiv.org/abs/1303.2559`).

Girault, V. and Raviart, P.-A. (1986). *Finite Element Methods for Navier–Stokes*. Springer-Verlag, Berlin.

Groß, S. and Reusken, A. (2011). *Numerical methods for two-phase incompressible flows*, volume 40 of *Springer Series in Computational Mathematics*. Springer-Verlag, Berlin.

Hysing, S., Turek, S., Kuzmin, D., Parolini, N., Burman, E., Ganesan, S., and Tobiska, L. (2009). Quantitative benchmark computations of two-dimensional bubble dynamics. *Internat. J. Numer. Methods Fluids*, **60**(11), 1259–1288.

James, A. J. and Lowengrub, J. (2004). A surfactant-conserving volume-of-fluid method for interfacial flows with insoluble surfactant. *J. Comput. Phys.*, **201**(2), 685–722.

Khatri, S. and Tornberg, A.-K. (2011). A numerical method for two phase flows with insoluble surfactants. *Comput. & Fluids*, **49**(1), 150–165.

Lai, M.-C., Tseng, Y.-H., and Huang, H. (2008). An immersed boundary method for interfacial flows with insoluble surfactant. *J. Comput. Phys.*, **227**(15), 7279–7293.

Muradoglu, M. and Tryggvason, G. (2008). A front-tracking method for computation of interfacial flows with soluble surfactants. *J. Comput. Phys.*, **227**(4), 2238–2262.

Pozrikidis, C. (2004). A finite-element method for interfacial surfactant transport, with application to the flow-induced deformation of a viscous drop. *J. Engrg. Math.*, **49**(2), 163–180.

Renardy, Y. Y., Renardy, M., and Cristini, V. (2002). A new volume-of-fluid formulation for surfactants and simulations of drop deformation under shear at a low viscosity ratio. *European J. Mech. B Fluids*, **21**(1), 49–59.

Schmidt, A. and Siebert, K. G. (2005). *Design of Adaptive Finite Element Software: The Finite Element Toolbox ALBERTA*, volume 42 of *Lecture Notes in Computational Science and Engineering*. Springer-Verlag, Berlin.

Teigen, K. E. and Munkejord, S. T. (2010). Influence of surfactant on drop deformation in an electric field. *Phys. Fluids*, **22**(11), 112104.

Teigen, K. E., Li, X., Lowengrub, J., Wang, F., and Voigt, A. (2009). A diffuse-interface approach for modeling transport, diffusion and adsorption/desorption of material quantities on a deformable interface. *Commun. Math. Sci.*, **7**(4), 1009–1037.

Xu, J.-J., Li, Z., Lowengrub, J., and Zhao, H. (2006). A level-set method for interfacial flows with surfactant. *J. Comput. Phys.*, **212**(2), 590–616.

Xu, J.-J., Yang, Y., and Lowengrub, J. (2012). A level-set continuum method for two-phase flows with insoluble surfactant. *J. Comput. Phys.*, **231**(17), 5897–5909.

Xu, J.-J., Huang, Y., Lai, M.-C., and Li, Z. (2014). A coupled immersed interface and level set method for three-dimensional interfacial flows with insoluble surfactant. *Commun. Comput. Phys.*, **15**(2), 451–469.

Yang, X. and James, A. J. (2007). An arbitrary Lagrangian–Eulerian (ALE) method for interfacial flows with insoluble surfactants. *FDMP Fluid Dyn. Mater. Process.*, **3**(1), 65–95.